1996

The effect of blend morphology on fracture toughness of rubber-modified epoxies

Ying-Chieh Huang
Lehigh University

Huang, Ying-Chieh

The Effect of Blend Morphology on Fracture Toughness...

October 13, 1996

THE EFFECT OF BLEND MORPHOLOGY ON FRACTURE TOUGHNESS OF RUBBER-MODIFIED EPOXIES

by

Ying-Chieh Huang

A Thesis

Presented to the Graduate and Research Committee

of Lehigh University

in Candidacy for the Degree of

Master of Science

in

Materials Science and Engineering

Lehigh University

October, 1996

CERTIFICATE OF APPROVAL

This thesis is accepted and approved in fulfillment of the requirements for the Master of Science.

September 27, 1996

Date

Thesis Advisor:

R. A. Pearson

Chairperson of Department:

D. B. Williams

ACKNOWLEDGMENTS

I would first like to thank my thesis advisor, Dr. Raymond A. Pearson for his advice, guidance, kindness, understanding, and support through this research. His literary support and valuable advice were very helpful to me.

I would like to express my great appreciation to Dr. Reza Bagheri for his very helpful discussions and assistance during this research.

I would also like to thank other colleagues at Polymer Interfaces Center and Polymer Engineering Laboratory who all have contributed in some manner, especially Dr. M. El-aasser, Dr. V. Dimonie, Jason Goodelle, Jenchou Hsiung, Guldem Guven, and Siriwan Phattanarudee. Technicians Dave Ackland, Arlan Benscoter, Gene Kozma, Andrea Pressler, Kathy Repa, and Jack Williams were also of great help and I thank them all.

The financial support provided by Polymer Interfaces Center is greatly appreciated.

Finally, I would like to acknowledge my parents, Cheng-Tzer Huang and Mei-Fen Shieh, for their support and encouragement. I also appreciate my sister and brother for their support through this research.

TABLE OF CONTENTS

LIST OF TABLES

LIST OF FIGURES

ABSTRACT

Epoxies are the mostly used and studied thermosetting materials with a very wide range of industrial applications. However, neat epoxies have low resistance to crack initiation and propagation. Addition of a second rubbery phase has been used to increase the toughness of these materials. Although the toughening effect has been modelled by many researchers, there is still no predictive model available for rubber-toughened epoxies that considers the effect of blend morphology. The morphology of the dispersion of the rubber particles in the epoxy matrix has been shown to be very important to the toughness performance, but only qualitative information is available. More understanding is needed.

In Chapter 1, some results of the influence of the morphological parameters of rubber-toughened plastics in the literature are summarized. The Objective and the Experimental Approach are discussed in Chapter 2 and 3, respectively. Chapter 4 shows the details of the experimental procedure and results. A summary and recommendation for this research are found in Chapter 5.

In this research, two model systems to further research the influence of the dispersion of the rubber particles to the toughness of the rubber-toughened epoxies have been developed. Both system use emulsification methods to control the overall blend morphology. One addresses the connectivity issue, and the other one addresses the clustering issue. The results show that the connectivity of the rubber particles may indeed be very important to the fracture toughness of the rubber-toughened epoxies. The results are preliminary and more control to the model systems is needed to further correlate the dispersion of the rubber particles to the fracture toughness performance of the rubber-modified epoxies.

1. INTRODUCTION

Epoxy polymers have been increasingly used as adhesives and as matrices for fiber-reinforced composites because of their outstanding mechanical and thermal properties such as high strength, high modulus, and high glass-transition temperature. However, pure epoxies have low resistance to crack initiation and propagation. It is very important to increase the toughness of these materials without causing any major losses in the other properties. Incorporation of a second phase of dispersed rubbery particles into these polymers can greatly increase their toughness without a significant loss of the other important properties.

It has been shown that morphology of these two-phase systems significantly influences the mechanical performance[1-3]. However, there are few quantitative studies of the relationships between blend morphology and mechanical properties because of the difficulty in estimation of regularity or randomness of morphology and the lack of a synthetic means to systematically vary morphological parameters, such as particle concentration, particle size, particle size distribution, interparticle distance, and particle dispersion. Reviews of these morphological parameters are briefly summarized in Section 1.1. Section 1.2 includes some morphology quantification methods and introduces a method developed recently for the correlation of the blend morphology with fracture toughness.

1.1 MORPHOLOGICAL PARAMETERS OF RUBBER-MODIFIED PLASTICS

1.1.1 Rubber Concentration

The toughness of a rubber-toughened plastic generally increases as the concentration of dispersed rubbery phase is increased. This tendency has been reported by many investigators[1,3,4-13]. The probably reason for this tendency is that the particle-particle interaction increases with rubber content[4]. However, there exists a maximum achievable toughness.

Bagheri[8] used MBS and CTBN rubber toughened DGEBA epoxy cured with piperidine and showed that the fracture toughness increases as concentration of rubber increases and then exhibit a plateau or slightly decline after the maximum. The results are showed in Fig.1-1. The optimum concentration might be due to the fact that at high rubber contents, not much matrix material is available for absorbing the fracture energy[1].

Kinloch and Hunston[7,12] used the concept of time-temperature superpositioning to separate the effects of changing the concentration and the properties of the matrix phase and claimed that there is no one unique relationship between toughness and the concentration of rubbery particles. These researchers demonstrated that the relationship between toughness and concentration of rubbery particles depends on the value of t_f/a_T(t_f is the time to failure and a_T is the time-temperature shift factor). This means that the relationship between fracture toughness and concentration of rubbery particles depends greatly on the test conditions[12].

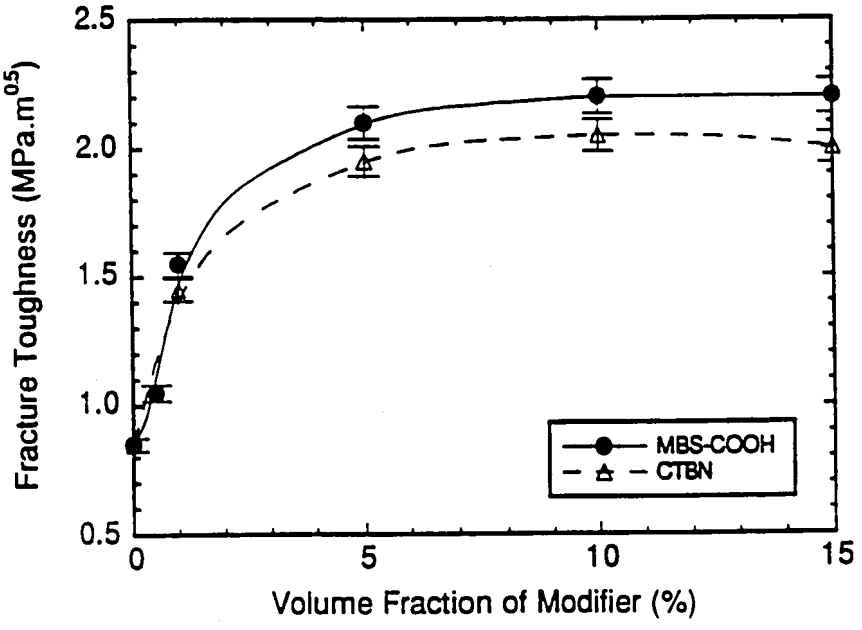

Fig. 1-1 Fracture toughness versus volume fraction of rubber particles in DGEBA epoxy cured with AEP. The fracture toughness increases as concentration of rubber increases and then exhibit a plateau or slightly decline after the maximum.[1]

1.1.2 Rubber Size

Wu[14] found that the notched impact toughness of rubber-toughened nylons increases as the size of the rubber particles decreases. This researcher claimed that the smaller the rubber particles the better for the fracture toughness[14]. However, Sultan and McGarry[15] have shown that 40nm particles are not as efficient as larger, 1μm particles in improving the fracture toughness of the epoxy resin. Wu[14] found that a sharp tough-brittle transition occurs at a critical particle size for a given rubber content and constant adhesion for nylon/rubber blends. The critical particle size was related to the rubber volume fraction ϕ_r by

$$d_c=\tau_c[(\pi/6\phi_r)^{1/3}-1]$$

where d_c is the critical rubber particle diameter, and τ_c is the critical surface-to-surface interparticle distance. When the average particle size is smaller than d_c, a blend is tough; when larger than d_c, brittle. The critical particle size d_c depends on the amount of rubber i.e., decreasing with decreasing the amount of rubber[16]. In other words, if the rubber particles are large, larger amount of rubber will be needed to achieve toughing, and vice versa[16].

Pearson and Yee[4] concluded that the effect of rubber particle size on fracture toughness is not significant based on a 0.2~5μm range of particle sizes. In a later publication[17], these researchers found that the fracture toughness is very dependent on particle size when the particles exceed 10μm in diameter. Table1-1 lists the fracture toughness values of some rubber-modified epoxies[17]. It suggests that fracture toughness increases with decreasing particle size. These researchers concluded that relatively large particles provide only a modest increase in fracture toughness by a particle bridging/crack deflection mechanism. In contrast, smaller particles provide a significant increase in fracture toughness by cavitation-induced shear banding[17]. At present, the optimal rubber particle size for toughing epoxies is in the 0.1~5.0 μm range[12,17,18].

Table 1-1 Fracture toughness values of some rubber-modified epoxies[17]

Formulation	**Particle size** (μm)	**K_{IC}** (**Mpa.m$^{1/2}$**)	**G_{IC}** (**J m^{-2}**)
DGEBA/PIP	0 (neat resin)	0.80	180
DGEBA/PIP/CTB-162	200	1.10	410
DGEBA/PIP/CTB/CTBN	1-2, 100-200	1.95	1275
DGEBA/PIP/CTBN-8	1-2	2.10	1440
DGEBA/PIP/CTBN-31	1-2, 10-20	2.00	1300
DGEBA/PIP/MBS	~0.2	2.90	2725
DGEBA/PIP/MBS/CTBN	0.2, 1-2	2.75	2465

Note: all rubber-modified epoxies contain 10 phr. rubber.

1.1.3 Rubber Size Distribution

The evidence concerning the influence of particle size distribution on measured toughness is somewhat contradictory. Riew and Bascom[19] have shown that a bimodal distribution of particle sizes enhances epoxy polymer toughness more than a mono-dispersed formulation. These researchers claimed that the large particles have induced localized shear yielding and that this yielding is facilitated by the presence of the smaller elastomer particles[19]. Pearson and Yee[17] questioned the "synergistic effect," since the investigators[19] used bisphenol A to obtain the bimodal particle size distribution and bisphenol A also acts as a chain extender, hence improving the toughenability of the matrix. Pearson and Yee[17] have found that there is some evidence of interactions between bridging particles(large particles) and cavitating particles(small particles), but no synergistic toughening was observed.

Chen and Jan[20] used two kinds of reactive liquid rubbers, CTBN1300×9 and CTBN1300×13, to modify Epon 828 epoxy resin. Piperidine was used as the curing agent. These researchers[20] attempted to keep the matrix property and total rubber content constant, while varying the relative amounts of large and small rubber particles and observed that the toughened systems with bimodal rubber particle size distribution can dissipate more strain energy through higher values of stress and elongation after yielding, i.e. they are more resistant to break through the formation of a localized shear yielding. Fig. 1-2 shows the dependence of fracture energy on rubber composition. These researchers claimed that the role of the small particles and the role of the large particles work by different mechanisms and that an interaction exists. The interaction gives rise to a synergistic toughening effect for the bimodal rubber particle distributed epoxy system[20].(Note that the average diameter of CTBN 1300×9 is 1.35 μm and the average diameter of CTBN 1300×13 is 0.2 μm.)

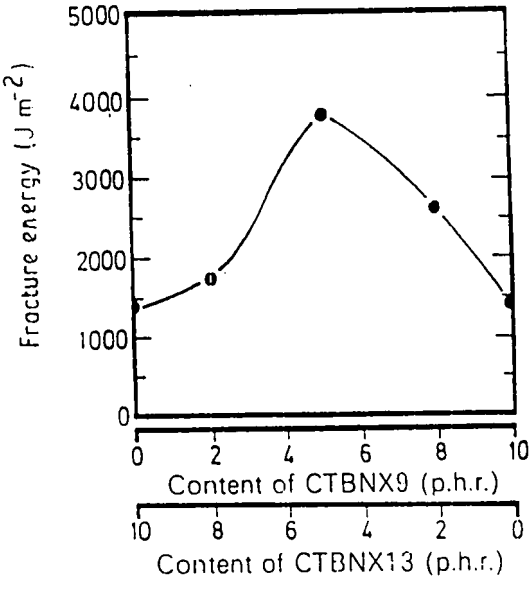

Fig. 1-2 Dependence of fracture energy on rubber composition for CTBN 1300×9 and CTBN 1300×13 mixed toughened epoxy resins. The toughened systems with bimodal rubber particle size distribution can dissipate more strain energy.[20]

1.1.4 Interparticle Distance (ID)

Interparticle distance has been reported by some investigators as an important parameter to the brittle-to-tough transition of rubber-modified plastics[6,8,14,16,21,22]. Wu[14] found that the brittle/tough transition of rubber/nylon blend occurs at a critical surface-to-surface interparticle distance. The ID is independent of the size and volume fraction of rubber and is a characteristic property of the matrix at a given mode, rate, and temperature of deformation[21]. That is, a polymer-rubber blend will be tough, when the ID is smaller than the critical value. A polymer-rubber blend will be brittle, when the ID is greater than the critical value[14]. Wu[14] attributed this phenomenum to stress field around isolated particles. When the particles are significantly close together, the stress field is no longer additive, and the field around neighboring particles will interact considerably[14].This will result in enhanced matrix yielding, and a transition to tough behavior[14].

Bagheri and Pearson[1], used different rubber modifiers to toughen epoxies and found that the transition in fracture toughness occurs at different ID for different modifiers. In other words, there is no specific ID in which the brittle/tough transition occurs[1]. Fig. 1-3 illustrates the fracture toughness data versus ID for modified epoxies. These researchers[1] proposed that the fracture toughness(K_{IC}) and the ID are correlated via a power law in the transition region :

$$K_{IC} = a \times (ID)^m$$

where "a" and "m" are constant parameters and vary with different modifiers. "m" has an almost value of -0.5 regardless the type and size of the modifier. "a", however, increases with the particle size. These researchers[1] believed that the brittle-to-tough transition is a kind of plane strain/plane stress transition. In other words, a ligament between two particles experiences a transition from plane strain to plane stress state by decreasing the ID. This conclusion is the same as what claimed by Borggreve et al.[6].

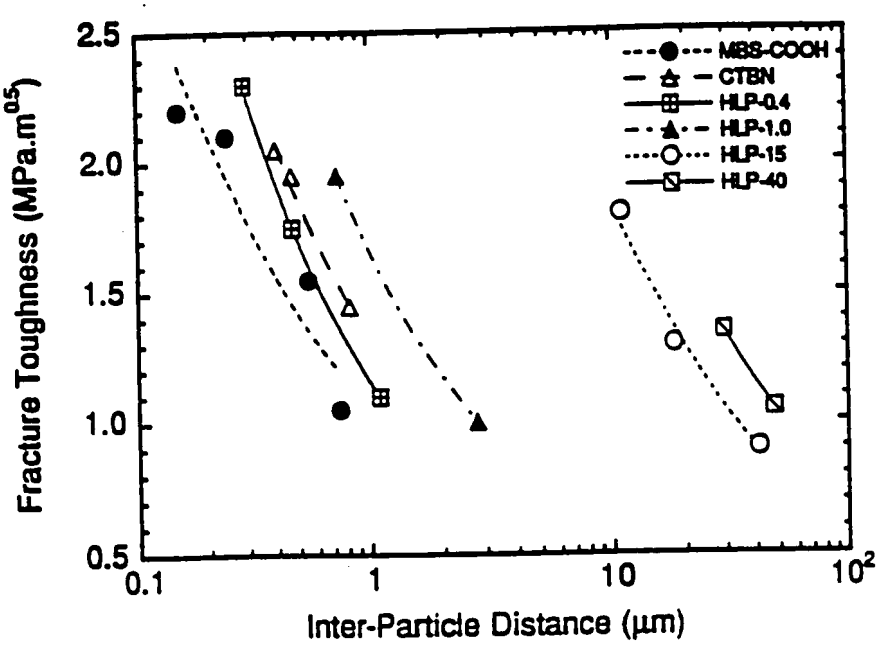

Fig. 1-3 Transition in fracture toughness versus inter-particle distance in modified blends. The transition in fracture toughness occurs at different ID for different modifiers.[1]

1.1.5 Dispersion of Rubber Particles

The dispersability of rubber in the epoxy has been reported by many investigators[1-3,23,24] as an important parameter to fracture toughness. Yamanaka et al.[23-24] obtained two types of particle dispersion, i.e. uniformly dispersed and inter-connected morphology via controlling the curing schedule. These researchers showed that a higher peel strength and damping efficiency of the inter-connected structure compare to that of the discrete morphology and predicted that the inter-connected structure may further enhances shear deformation in a rubber-modified epoxy[24]. Fig. 1-4 is a schematic representation of inter-connected structure.

Huang[3] developed two spatial parameters, normalized interparticle distance index and relative angle index, and used Finite Element Method(FEM) to develop a distribution profile and an energy absorption index. Through the energy absorption index, one can successfully correlate the morphology with the toughness performance[3]. This researcher concluded that the optimal dispersion pattern for low rubber concentration(lower than 10%) blends is uniform dispersion and inter-connected morphology is desired for high rubber concentration[3]. However, Bagheri[1] disproved it since he found that the low rubber content blends still show higher fracture toughness with an inter-connected morphology and the greater the inter-connected the higher the fracture toughness.

Qian[2] synthesized custom core-shell rubber particles to toughen epoxies and found that the degree of particle dispersability in the epoxy matrix plays a crucial role in toughening of epoxies. A higher degree of segregation(clustering) of the particles in the epoxy matrix yields a higher fracture toughness of the modified epoxies[2]. Fig. 1-5 is a representation of the formation of the "clustering" in the epoxy matrix. Before curing, the PMMA shell was miscible with liquid epoxy, and the PMMA chains and epoxy molecules interdiffused into each other. Entanglements of the PMMA chains can also take place between the particles[2]. During curing, the miscibility between the PMMA shell and the curing epoxy decreased and

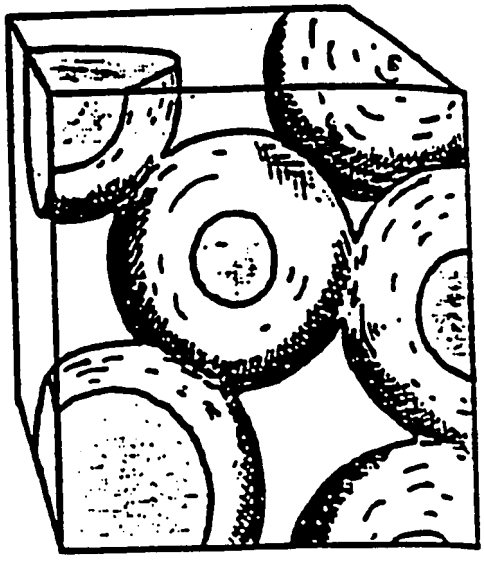

Fig. 1-4 Schematic representation of inter-connected structure[24]

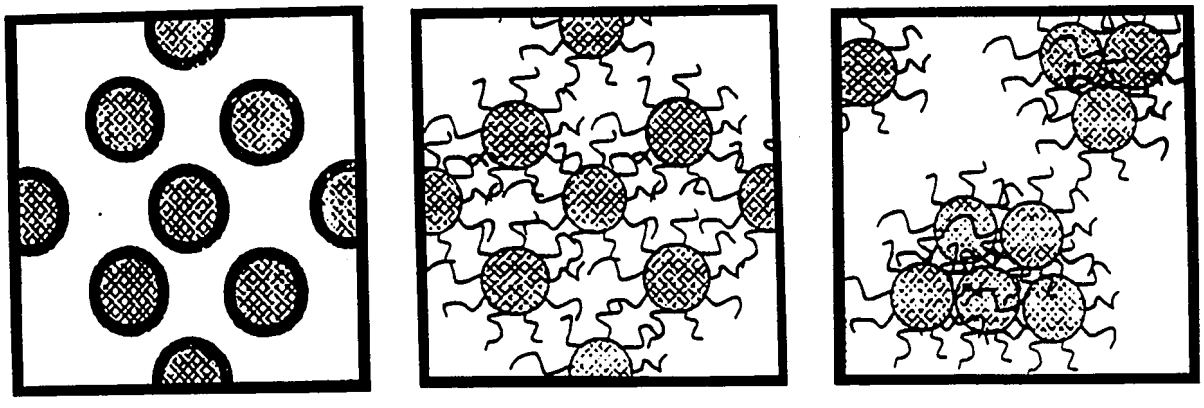

(A) Core/Shell Particles

(B) Extended particles in Epoxy (before curing)

(C) Segregated particles in Epoxy (after curing)

Fig. 1-5 Schematic representation of "cluster" formation mechanism during the epoxy curing : A) original core/shell latex particles ; B) extended particles in the epoxy before curing ; C) segregated particles in the epoxy after curing[2]

caused the phase separation of rubber from matrix and formed the "clusters"[1-2]. These researchers[1-2] showed that the degree of dispersability can be changed by changing the chemistry of the shell, the type of curing agent, and the mixing procedure.

Some mechanisms responsible for the superior fracture toughness of inter-connected morphology have been proposed[3,16,23]. Wu[16] applied the percolation concept to the rubber-toughened nylon system and concluded that the higher fracture toughness provided by the inter-connected structure was due to its lower percolation threshold. Yamanaka et al.[23] predicted that the shear yielding of the epoxy might be enhanced by the co-continuous morphology. The schematic diagram of this concept is represented in Fig.1-6. A cooperative cavitation of the particles would be formed in front of the crack tip due to the clustering morphology of the particles in the epoxy matrix; while in the case of the epoxy with a uniform dispersed morphology, a random cavitation of the particles is formed. Therefore the size of the plastic zone in the modified epoxy with a clustering morphology should be much larger than that of the modified epoxy with a uniform dispersed morphology and thus results a much higher fracture toughness of the epoxy. This propose was confirmed by Bagheri[1] and Qian[2].

Fig. 1-7 a and b represent the TOM micrographs taken from the crack tip damage zone of MBS and MBS-COOH modified epoxies respectively. (Note that the blend morphologies for them are inter-connected and uniformly dispersed respectively, as shown in Fig. 1-8 a and b). As seen in the figures, the blend with an inter-connected morphology has a significantly larger plastic zone size than the blend with a uniformly dispersed morphology. Thus the superior fracture toughness performance of the inter-connected morphology can be explained.

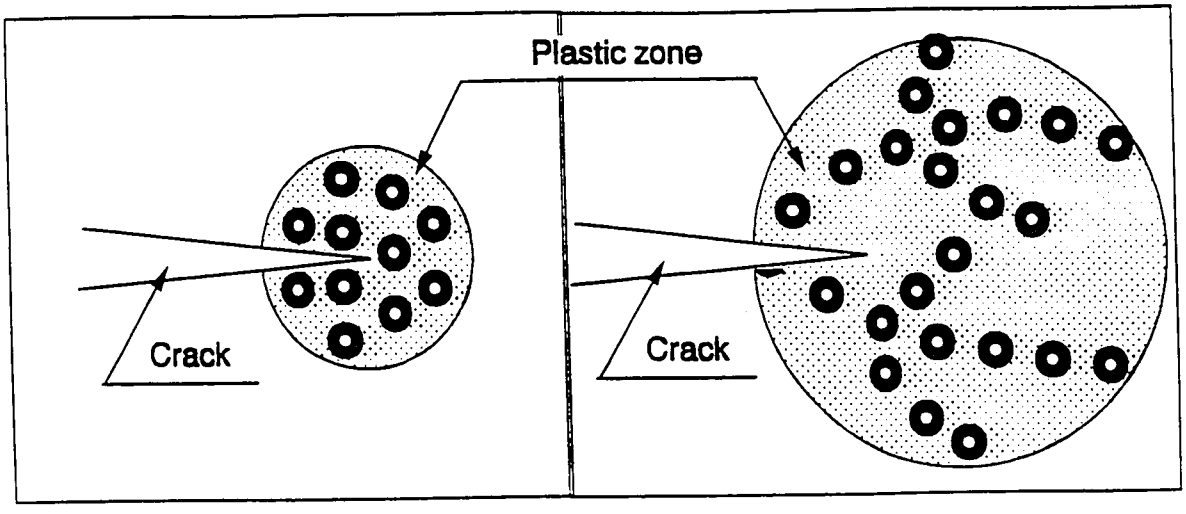

Fig. 1-6 Schematic diagram of the plastic zone in the modified epoxy with (A) a uniform particle dispersed morphology and (B) a micro-clustering morphology[2]

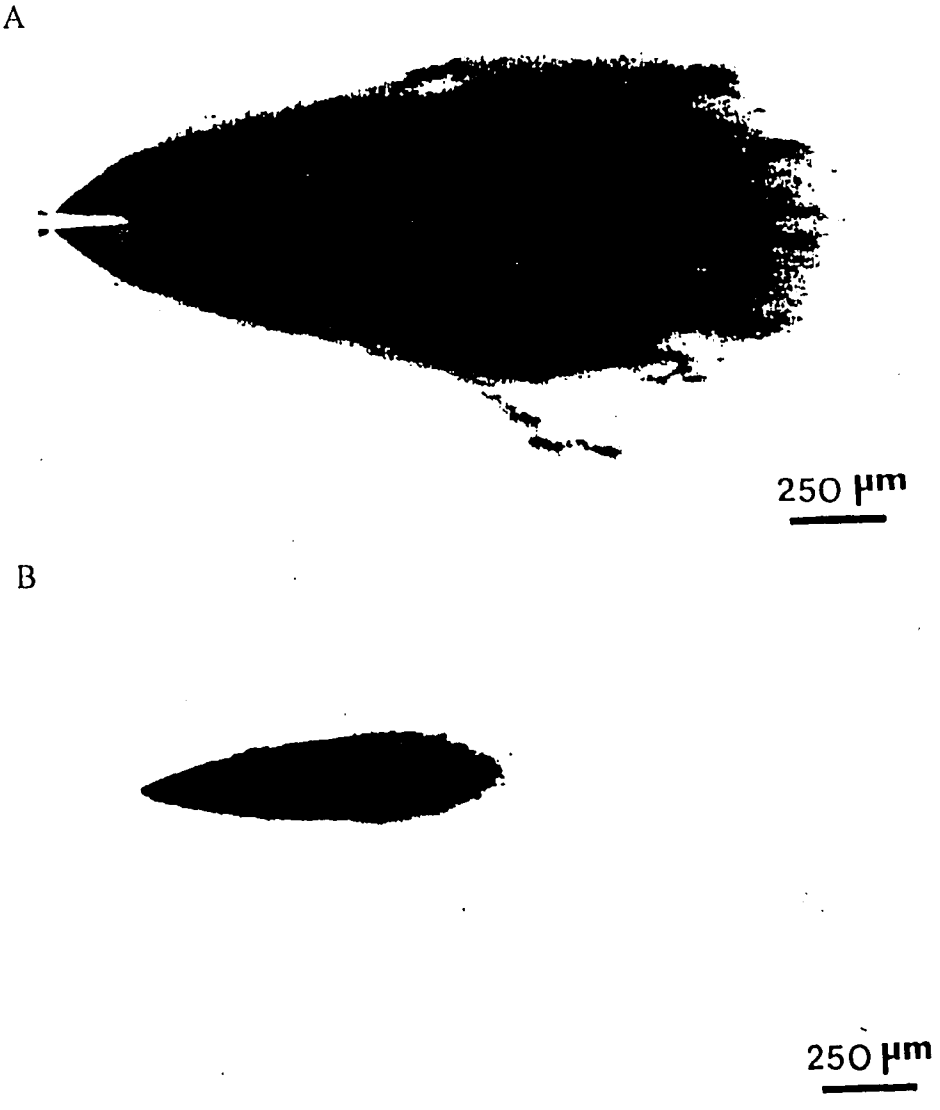

Fig. 1-7 The TOM micrographs taken from the crack tip damage zone of piperidine-cured epoxies which are modified by 10wt% of (a) MBS and (b) MBS-COOH particles. As seen in these figures, the MBS-modified material has significantly larger plastic zone size than that of the MBS-COOH modified material.[1]

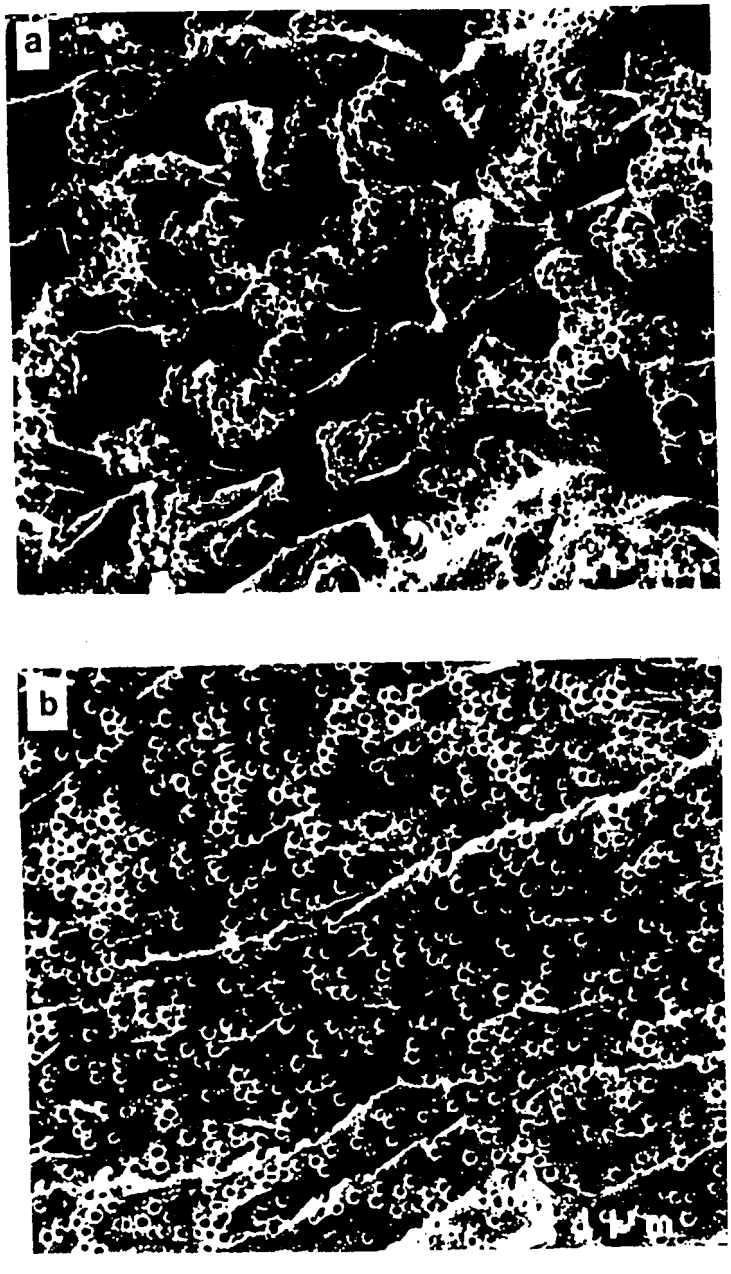

Fig. 1-8 SEM micrographs taken from the stress-whitened zone of piperidine-cured epoxies which are modified by 10wt% of (a) MBS and (b) MBS-COOH particles. As seen in these figures, particles that are dispersed uniformly in the presence of acid groups, have formed a continuous-like morphology in the absence of reactive groups.[1]

1.2 QUANTIFICATION OF MORPHOLOGY

Particle dispersion has been reasoned to be related to the local stress state and thus may affect the final failure mechanism[14,21]. But, attempts to correlate particle dispersion with any macroscopic mechanical properties have been severely hindered by the lack of constitutive models and suitable quantitative parameters. The quantitative analysis of a spatial distribution are summarized in 1.2.1 and 1.2.2. The correlation of distribution with mechanical properties is summarized in 1.2.3.

There are several mathematical methods to extract the information on the spatial distribution of points in a pattern.

1.2.1 Special Functions Characterizing The Randomness[25]

(a) *P* function

P function is a cumulative distribution function of the distance between random points and the nearest object r_1. The *P* function P(t) is defined by

$$P(t) = Pr(r_1 < t)$$
$$= Pr(\text{random point is in the circles of radius t with center } x_i)$$
$$= S^{-1}(\text{area of union of circles of radius t which have the centers at each object})$$

Where Pr ( ) is the probability, S the total area, and x_i the coordinate of the ith point. The *P* function is a smooth function of t.

(b) Q function

Q function is a cumulative distribution function of the distance between two nearest-neighbor points r_2. The Q function is defined by

$$Q(t) = \Pr (r_2 < t)$$

Q(t) is not a smooth function of t, but it is more sensitive to the randomness than P(t).

1.2.2 Thiessen Tessellation

Thiessen polygons were first proposed by A. H. Thiessen[26], and later further developed by R. E. Horton[27]. Thiessen polygons are formed from drawing vertical bisectors of the lines joining any two particles. The smallest polygons encompassing each particle (or center) are defined as the Thiessen polygons, as shown in Fig. 1-9. All locations inside each polygon are closer to its center than to any other center, and the particles that share a common edge are call "Thiessen Neighbors", as shown in Fig. 1-10. The distribution profiles of the number of cell sides (number of Thiessen neighbors), the perimeter of the cell, and the area of the cell can all be used to represent the dispersion characteristics.

However, all the statistical parameters above are "scalar" and can only represent the deviation from random dispersions.

1.2.3 Normalized Interparticle Distance Index and Relative Angle Index

More recently, Huang[3] proposed two spatial parameters. One is the normalized interparticle distance index (Fig. 1-11), and the other is relative angle index (Fig. 1-12). This researcher calculated these two parameters of every pair of first neighbors to generate a normalized frequency distribution. Fig. 1-13 is the histogram of the normalized frequency distribution of a material. The x-axis is the interparticle distance index, Δ_{fn}, and the y-axis is the relative angle index, Θ_{fn}. The shade represents the frequency of a particular Δ_{fn} and Θ_{fn} interval; the lighter the shade, the higher the frequency is. The shade variation, in either direction, then represents the frequency distribution along that axis[3]. Huang[3] assumed that toughness, which is a macroscopic property and is interpreted as the ability to absorb energy, might be comparable to the sum of the local microscopic energy absorption events. This researcher argued that first neighbor interaction is the most dominant factor that influences the local stress state, thus the toughness should be proportional to the sum of all energy absorption events between all first neighbor pairs.

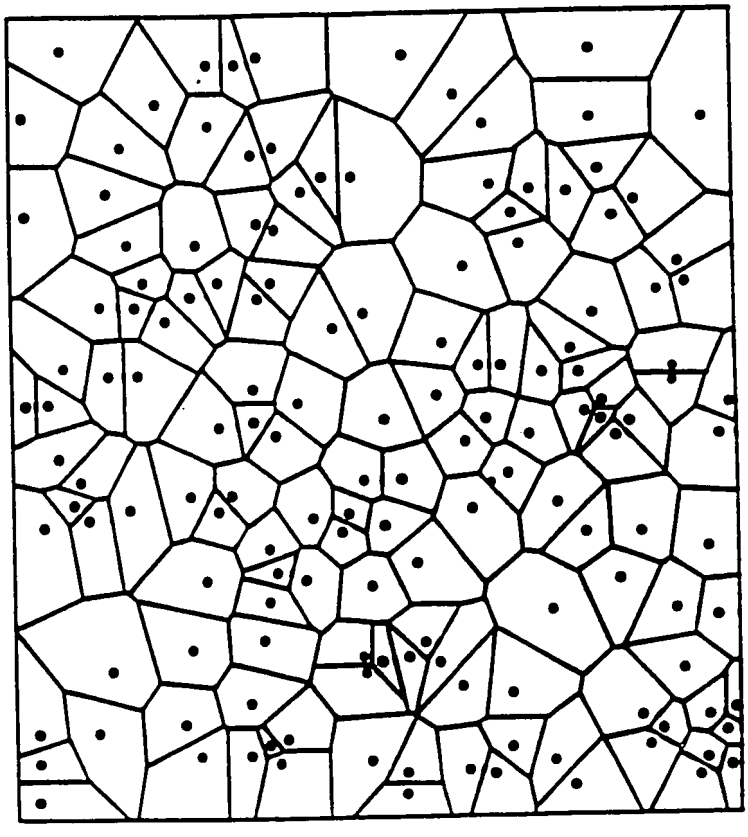

Fig. 1-9 Thiessen polygons[3]

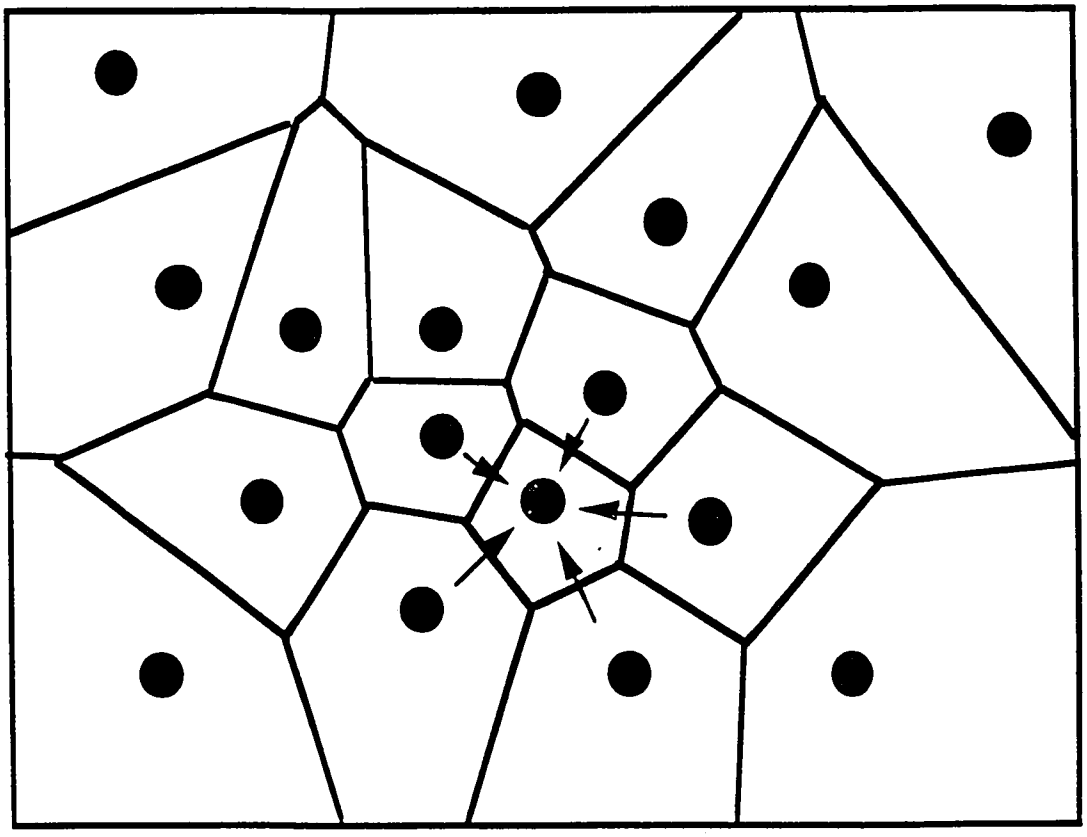

Fig. 1-10 Thiessen neighbors[3]

$$\Delta fn = (r1+r2) / L$$

where r = radius of each individual particle

L = distance between the centers of the particles

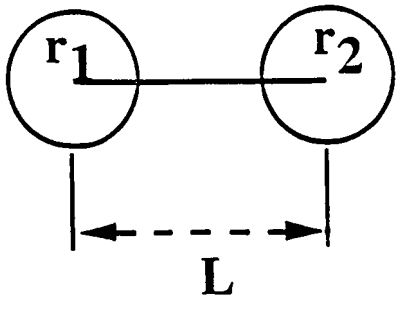

$$0 \leq \Delta fn \leq 1$$

Fig. 1-11 Normalized interparticle distance index[3]

$$\Theta_{fn} = \arctan\left(\frac{y_2 - y_1}{x_2 - x_1}\right)$$

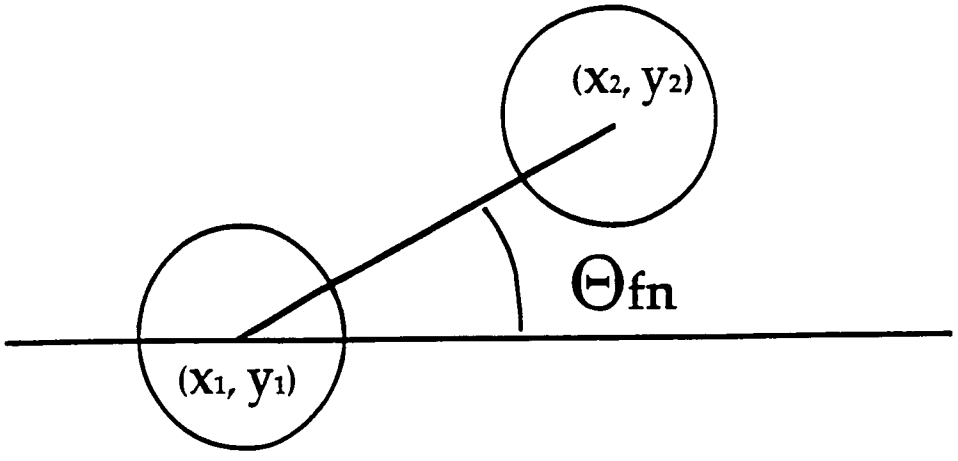

$$0^o \leq \Theta_{fn} \leq 90^o$$

Fig. 1-12 Relative angle index[3]

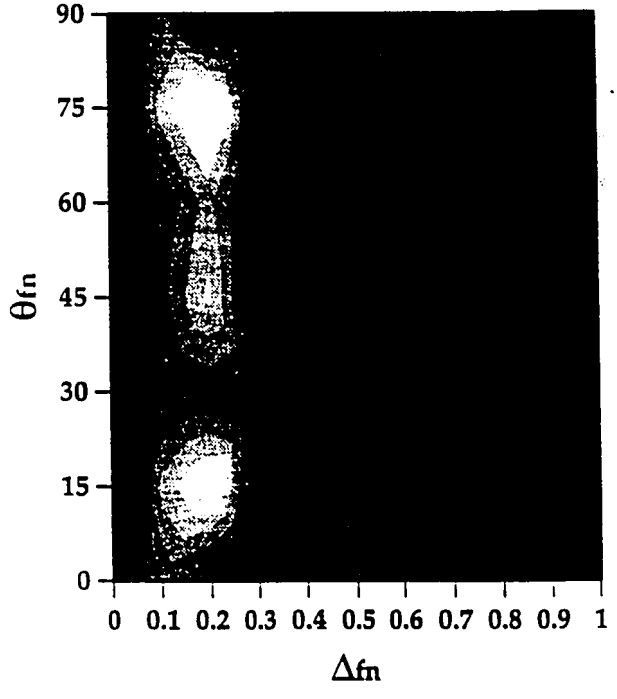

Fig. 1-13 2-D contour plot of a typical frequency distribution[3]

Huang[3] first determined the dispersion profile of a blend, in terms of the frequency distribution of Δ_{fn} and Θ_{fn}. Then used FEM technique to characterize the energy absorption between a pair of first neighbor particles. Afterward, the overall energy absorption potential for a particular blend can be determined from a compilation of the local strain energy absorption indices and the frequency distribution of Δ_{fn} and Θ_{fn} of the blend.

The overall energy absorption index (Σ) can be mathematically represented by

$$\Sigma = \sum_{\Delta fn=0}^{1} \sum_{\Theta fn=0^\circ}^{90^\circ} (D_{\Delta fn,\Theta fn} \times E_{\Delta fn,\Theta fn})$$

$D_{\Delta fn,\Theta fn}$ is the spatial distribution profile of the particles in a blend. $E_{\Delta fn,\Theta fn}$ is the energy absorption profile of different spatial arrangements. Fig. 1-14 shows the overall energy absorption index (Σ) versus concentration for epoxy/EXL-2691 blends. The trend of Σ is consistent with the trend of the fracture toughness.

It seems that through the energy absorption index, one can successfully correlate the morphology with the toughness performance, but it only suggests an optimization of the toughness with a given concentration of toughener particles. Further developments are needed to predict the toughening performance of a polymer blend.

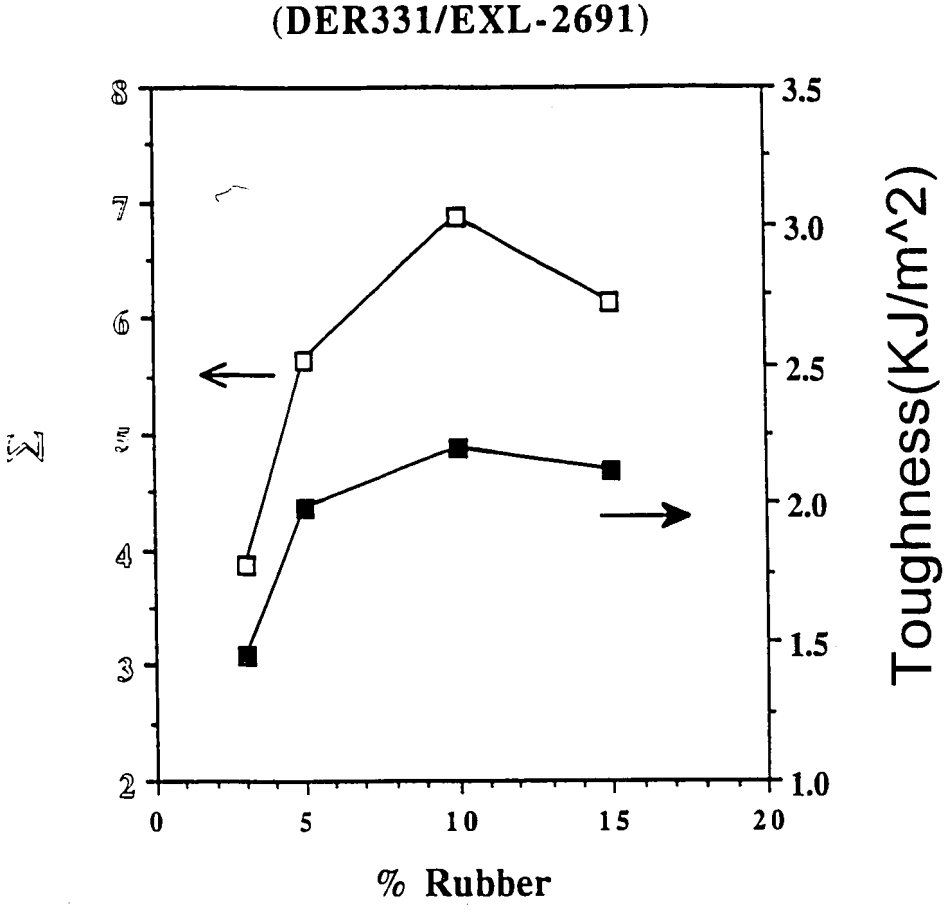

Fig. 1-14 Overall energy absorption potential versus particle concentration for the epoxy/EXL-2691 blends. The trend of energy absorption index is consistent with the trend of the fracture toughness.[3]

2. OBJECTIVE

The morphology of the dispersion of the rubber particles has been shown that as an important parameter that influences the fracture toughness of the blend[1-2]. However, quantitative correlation between the morphology with toughness performance has not been performed. The next most important step is to characterize the particle dispersion and establish a quantitative correlation with the overall toughing performance.

Qian[2] proposed that in order to understand the effect of dispersion morphology to the toughening performance, it is desirable to precisely control the degree of the segregation. This can be achieved by emulsification of the uncured epoxy. The size of the epoxy particles and number of the particles within each epoxy particle might be controlled by the degree of emulsification and ratio of the rubber particles and epoxy. Thus we proposed some model systems which are described in Fig.2-1.

Fig. 2-1 (A) is the description of the original system in which the rubber particles disperse uniformly. Fig. 2-1 (B) is the description of the first model system which uses pre-gelled epoxy particles to force the rubber particles segregate. Fig . 2-1 (C) is the description of the second model system which uses rubber particles imbedded in pre-gelled epoxy particles to control the micro-clusters of the rubber particles. Both systems can be achieved by emulsification. Through these model systems we may systematically vary the dispersion of rubber particles and then get some insight of the correlation between the dispersion of the rubber particles with toughness performance.

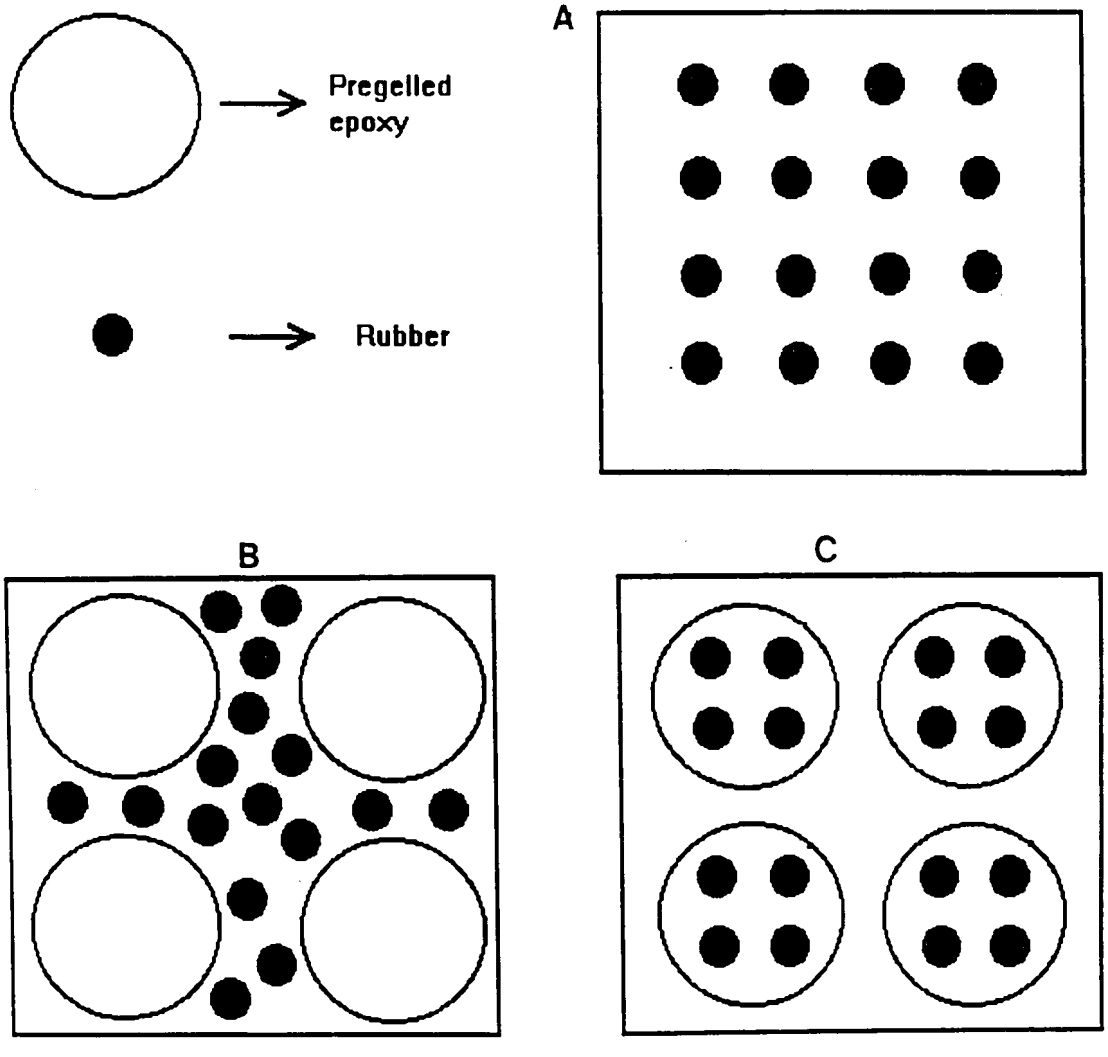

Fig. 2-1 Schematic representation of the proposed model systems[28]
(A) Randomly dispersed rubber particles(original system)
(B) Clustered but not connected(model I)
(C) Clustered and connected(model II)

3. EXPERIMENTAL APPROACH

3.1 MATERIAL PREPARATION

The epoxy resin used was DER331 (Dow Chem.), a liquid diglycidyl ether of bisphenol-A (DGEBA). Its properties are shown in Table 3-1. Piperidine (Fisher Scientific) was used as the curing agent. The molecular structures of the epoxy resin and the piperidine curing agent are shown in Fig. 3-1. Table 3-2 is the description of the toughing agents used.

Table 3-1 Typical properties of DER331 liquid epoxy resin[2]

n	Epoxide Equiv. Wt.	Viscosity (cps@25° C)	Color Max. (Grader)	Flash Point (° F)	Specific Gravity (25/25° C)
0.15	182-192	11,000-14,000	125*	485	1.16

* APHA Color --- ASTM method 1209

Table 3-2 Description of the modifier

Modifier	Description of Modifier
MBS	Structured core/shell latex particles comprised of a methacylated butadiene-styrene copolymer from Rohm&Haas[EXL-2691(25%shell), RJC-2680(60%shell)]
MBS-COOH	Similar to MBS plus the acid functionality in the PMMA shell from Rohm&Haas[EXL-2611]

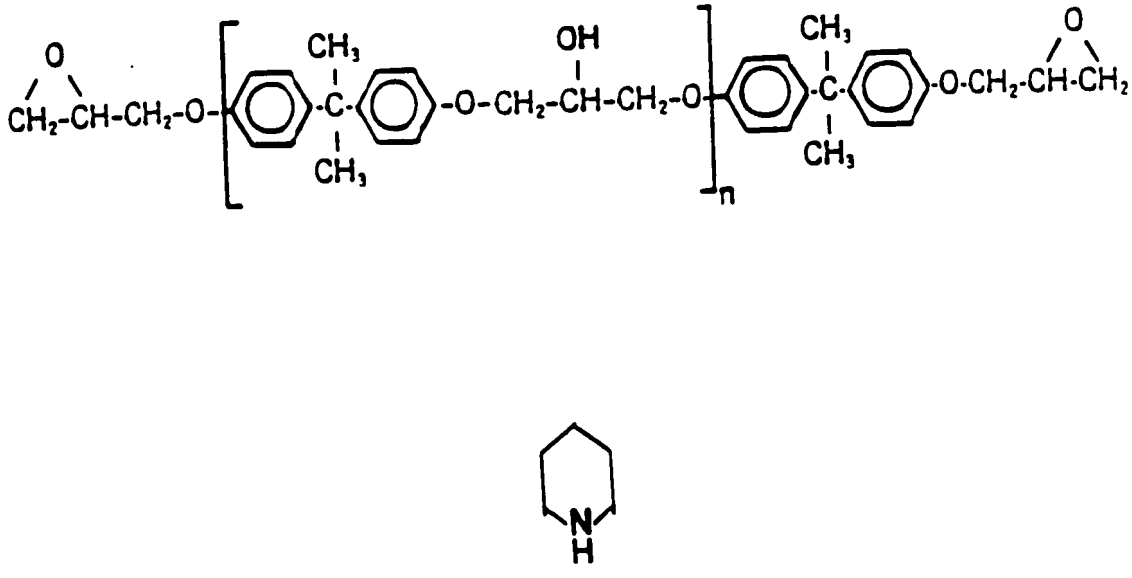

Fig. 3-1 The molecular structures of the epoxy resin[1] and piperidine curing agent[2]

3.1.1 Epoxy Systems

(A) The neat epoxy systems were first heated to 80°C in a silicone oil bath and degassed. 5 phr curing agent was then injected, mixed with epoxy, and degassed again. The liquid was then poured into a preheated (80°C or 120°C depends on the curing schedule) mold. The mold was then placed in an oven for the curing. After the curing, the mold was removed from the oven and allowed to cool gradually to room temperature.

(B) For MBS(EXL-2691) modified epoxies, the rubber was first mixed with the epoxy and followed the same cure procedure stated above.

(C) For MBS-COOH(EXL-2611) and MBS(RJC-2680) modified epoxies, a solvent-based process was used to disperse the rubber particles since the segregation could not be broken down by normal stirring[1-2]. The rubber particles was mixed with acetone at room temperature for at least 12 hours and then be sonified for 2 mins. Then the epoxy resin was added. The solvent was then removed by vacuum distillation at 80°C. After the solvent was completely removed, the cure procedure in **(A)** was used.

3.1.2 Rubber/Epoxy particles/Epoxy System(model I)

(A) Fabrication of Epoxy Particles

Table 3-3 is the recipe used which was developed from a technical report of the Emulsion Polymers Institute[29].

Table 3-3 Description of the recipe

Water Phase	DDI water : 150 g
	Hexadecyltrimethylammonium bromide : 0.67 g
	Cetyl alcohol : 1.36 g
Oil Phase	Epoxy(DER 331) : 25 g
	Toluene : 6.3 g
	Methyl isobutyl ketone(MIBK) : 6.3 g
	Piperidine : 1.5 c.c.

The oil phase was mixed at 80°C and then 5 phr curing agent was added. The oil phase was then mixed and then cured in an oven for the curing procedure(details will be discussed in section 4.1). The water phase was mixed at 80°C. After the curing, the oil phase was then dispersed into the water phase by mechanical stirring. The solvents and surfactant were removed by vacuum distillation(80°C) and repeated hot DDI (Distilled-Deionized) water extraction(50°C), respectively[30]. The liquid was then dried(50°C) in an oven to get the epoxy particles.

(B) Rubber/Epoxy particles/Epoxy System

The same procedures stated in section 3.1.1**(C)** was followed.

3.1.3 Epoxy Particles(with rubber particles in them)/Epoxy System(model II)

(A) Fabrication of epoxy particles

10wt% rubber particles was mixed with acetone at room temperature for at least 12 hours and then be sonified for 2 mins. Then the epoxy resin was added. After the solvent was totally removed by vacuum distillation at 80°C, the other elements of the oil phase(Table 3-3) were then added. Then the procedure in 3.1.2 **(A)** was used.

(B) Epoxy Particles(with rubber particles in them)/Epoxy System

The epoxy particles(with rubber particles in them) were added into the liquid epoxy and then followed the same procedure stated in section 3.1.1**(A)**.

3.2 CHARACTERIZATION TECHNIQUES

3.2.1 Light Scattering Particle Analysis

A Coulter N4MD sub-micron particle analyzer was used to observe the size and size distribution of the epoxy particles. A drop of the epoxy emulsion was put in a clear cuvette and diluted by water to a suitable concentration for observation.

3.2.2 Transmission Optical Microscope (TOM)

An Olympus BH-2 transmission-light microscope was used to observe the size and size distribution of the epoxy particles. A drop of the epoxy emulsion was spread onto a glass slide for the observation.

3.2.3 Fracture Toughness

A single-edge-notched 3 point bending (SEN-3PB) method was used to determine the average critical stress intensity factor K_{IC} of at least 5 specimens per formulation. The specimens were either generated by cutting from a plaque or by using a mold which was designed for 3PB specimen for casting. Fig. 3-2 illustrates the geometry used. The ASTM D5045[31] guideline was followed. Pre-cracks were introduced to the notched specimens by hammering a razor blade which was immersed in liquid nitrogen to generate a sharp crack.

The fracture toughness tests were performed using an Instron 1011 screw-driven Instron testing frame at a cross-head speed of 1mm/min. The following relations[1] were used to calculate K_{IC} :

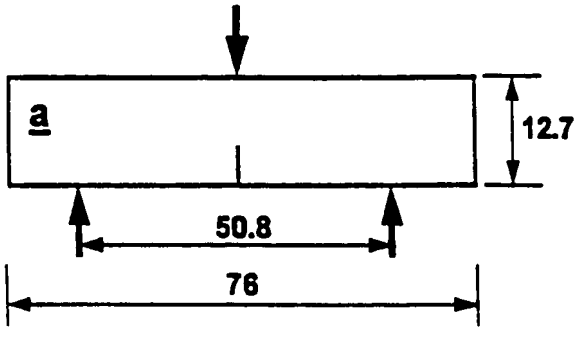

Fig. 3-2 Schematic diagram of geometry used for fracture toughness assessment[1]. All dimensions are millimeters.

$$K_{IC} = \frac{10^{3/2} \times P \times S}{t \times w^{3/2}} f(x)$$

$$f(x) = 3x^{1/2} \frac{[1.99 - x(1-x)(2.15 - 3.93x + 2.7x^2)]}{2(1+2x)(1-x)^{3/2}}$$

where P: critical load for crack propagation in kilo-newton

S: Span length in millimeter (50.8 here)

t: specimen thickness in millimeter

w: specimen width in millimeter

f(x): non-dimensional shape factor

x: a/w, the crack length to specimen width ratio

a: crack length in millimeter (measured after the specimen breaks)

3.2.4 Compression Test

The compressive behavior of materials were evaluated by the ASTM D695 test method[32]. 5×5×10 mm specimens were machined from the cured plaques. An Instron 1011 screw-driven Instron testing frame at a cross-head speed of 1.5 mm/min was used. The results are average of at least 3 tests.

3.2.5 Scanning Electron Microscope (SEM)

Fracture surface of the SEN-3PB specimens were examined using a JEOL 6300F scanning electron microscope at an acceleration voltage of 5kv. Samples were cut from the fractured specimens and coated with a thin layer of Au-Pd to reduce any charge build-up. Fig. 3-3 represents the fracture surface of the SEN-3PB specimen. As seen in the figure, three different deformation regions were formed. They are pre-crack region, slow crack growth

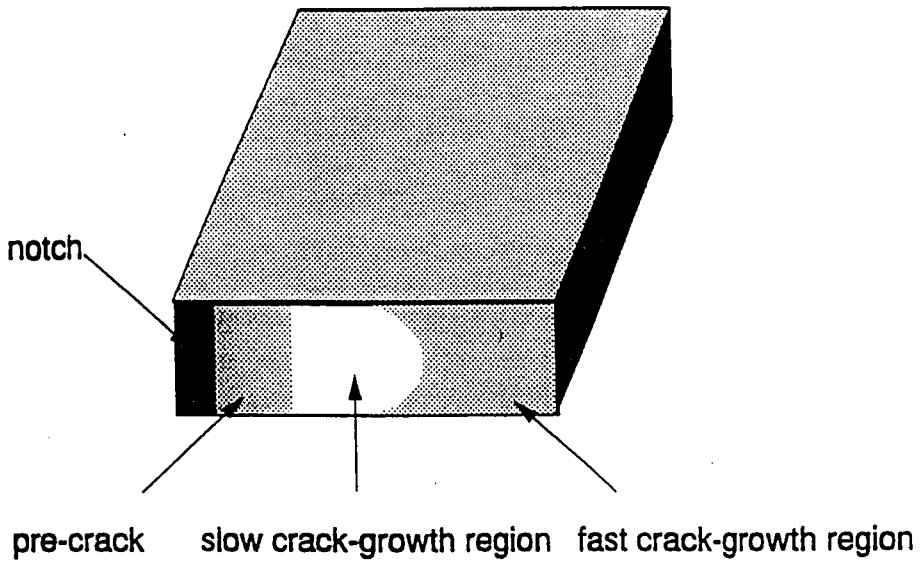

Fig. 3-3 Schematic representation of the fracture surface[2]

region(stress-whitened zone), and fast crack growth region. The SEM observations were performed in the slow crack growth region(stress-whitened zone) since it represents the plastic zone.

3.2.6 Differential Scanning Calorimetry (DSC)

Glass transition temperature (Tg) of neat and modified epoxies were measured using a Mettler TA 3000 Thermal Analysis System. Powder or a small piece from the specimens weighted 15~20 mg were used. DSC analysis were conducted at a heating rate of 10°C/min in the range of 0~150°C.

4. RESULTS AND DISCUSSION

4.1 EMULSIFICATION OF EPOXY

The epoxy particles were produced by a direct emulsification method[33]. The liquid epoxy is added to a mixture of water and volatile solvents and emulsified in water containing surfactant using conventional emulsification methods. The epoxy existed as small spherical droplets surrounded by surfactant which forms a "skin" over the droplets and thus prevented coalescence of the particles[34]. Since the curing agent is present the particles are allowed to gel. The solvent and surfactant were then removed by vacuum distillation and hot DDI water extraction respectively. The liquid was then dried in an oven to get the epoxy particles. Fig. 4-1 is a schematic drawing of the procedures of the making of the epoxy particles. As seen in Fig, 4-1, the oil phase and water phase were made separately first and then the oil phase was dispersed into water phase by mechanical stirring. The curing step of the oil phase was to confirm that the epoxy particles will not deform during the drying and the later steps. This will be discussed later.

As shown in Table 3-3, toluene and MIBK were used to lower the viscosity of the epoxy to a level suitable for emulsification. Hexadecyltrimethylammonium bromide and Cetyl alcohol acted as surfactants to stabilize the dispersed epoxy particles in the water.

Many batches were tried to develop this recipe because the amount of the solvents and surfactant significantly affect the particle size and size distribution. Some solvent is needed to lower the viscosity of epoxy but too much solvent will cause smaller particle size and increase the difficulty in the solvent removing step. The amount of surfactant is important also because too much will decrease the particle size and too little will decrease the stability of the dispersion.

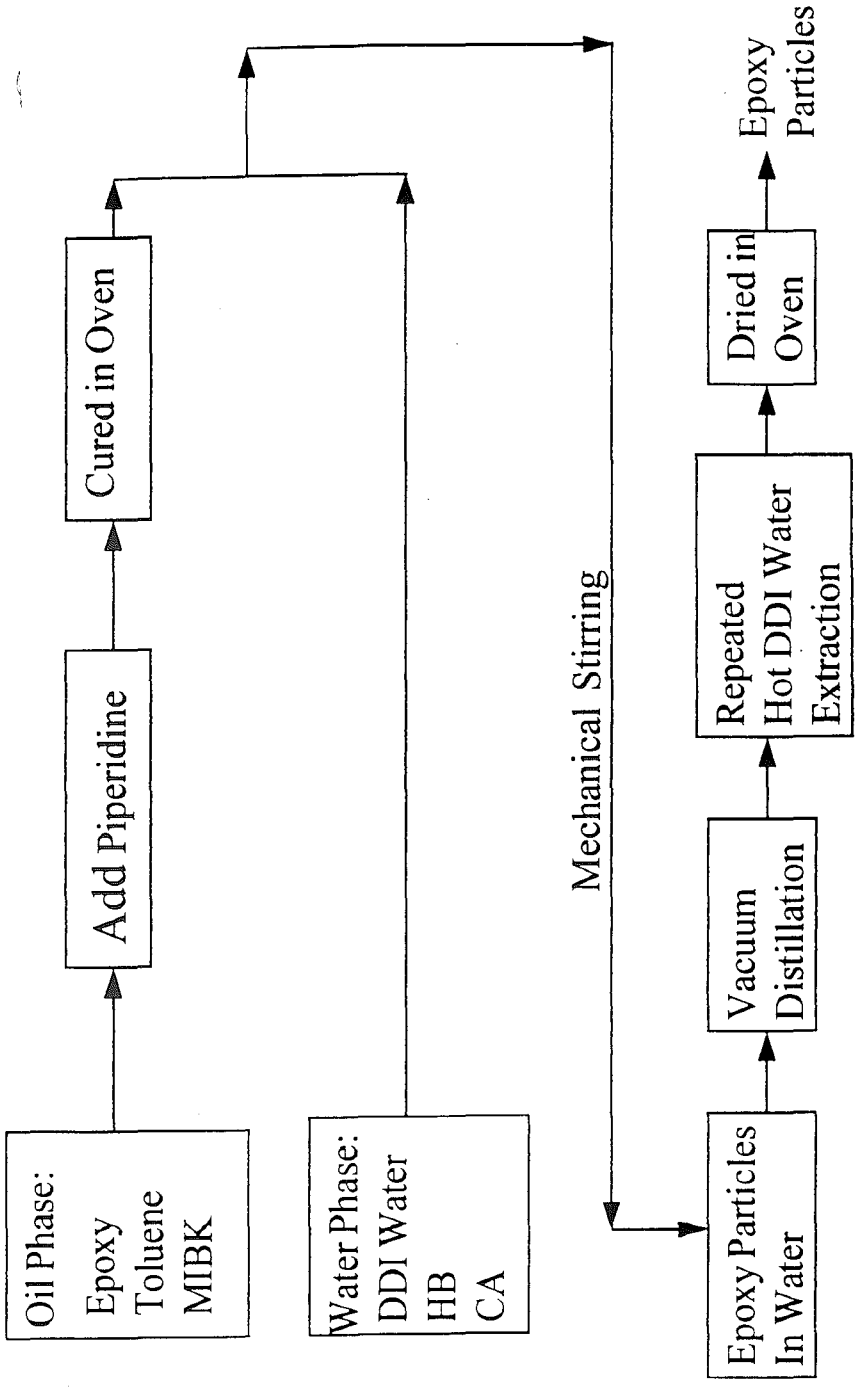

Fig. 4-1 Schematic drawing of the processing of the epoxy particles

Table 4-1 lists some representative batches tried. From batches **a** and **b**, we can know the effect of ultrasonification. Ultrasonification is always used for emulsification to generate small and narrow size distribution particles. However, a large particle size (larger than 5μm) is preferred for this study since such particles would be effective to promote the clustering of the 0.2μm rubber particles. Sub-micron epoxy particles can not effectively force the rubber particles to segregate. Thus only mechanical stirring can be used to disperse the oil phase and this results in large particles with a broad size distribution. In batch **c**, no solvent was used. The viscosity of epoxy increased rapidly after the adding of curing agent and it was impossible to use the spin bar to disperse the oil phase. Therefore some solvent must be used to lower the viscosity of the epoxy. In batch **d**, the dispersion coagulated. This result suggests more surfactant is necessary to stabilize the particles. In batch **e**, we used much larger amount of surfactant and the result was small particle sizes. The recipes for batch **f** and **g** were identical and the results were large particles and broad particle size distributions. The difference of the recipe for batch **h** with batch **f** and **g** was the curing schedule. The longer curing time can cause some very large particles. In batch **i**, the curing time was only 2 hours and the result was similar to that of batch **f** and **g**. These results suggest that 2 hours curing time is enough for our particle size requirements even though some sub-micron size particles will be generated. Fig. 4-2 is the TOM photograph of the epoxy particles generated in batch **h**. The particle size distribution is very broad, but we can get the suitable sizes we need for the next step (add these pre-gelled epoxy particles into rubber-modified epoxies to control the segregation of rubber particles). Fig. 4-3 is the TOM photograph of the epoxy particles generated in batch **i**. The size and size distribution are pretty similar to Fig. 4-2. One can use screen meshes to narrow the size distribution.

Table 4-2 shows the Tgs of the epoxy particles generated in batch **h** and **i**. It shows that the Tg of the epoxy particles increases as the curing time increases. It means that the crosslink density of the epoxy particles increases as the curing time increases.

Recipe **i** and 2 hours curing time were used for the fabrication of the epoxy particles in Section 4.3.

Table 4-1 Development of the recipe

Batch ID	Water (g)	HB (g)	CA (g)	Toluene (g)	MIBK (g)	Epoxy (g)	PIP (cc)	Curing Time(hr)	Sonify (min)	Size (μm)
a	150	0.67	1.36	12.6	12.6	25	1.5	1.6	2	0.326~0.357
b	150	0.67	1.36	12.6	12.6	25	1.5	2	1	0.306~0.345
c	150	0.22	0.45	0	0	25	1.5			*
d	150	0.22	0.45	6.3	6.3	25	1.5	2	0	**
e	150	1	2.04	6.3	6.3	25	1.5	2	0	0.207~0.352
f	150	0.67	1.36	6.3	6.3	25	1.5	4	0	14~35.6
g	150	0.67	1.36	6.3	6.3	25	1.5	4	0	8.9~35.9
h	150	0.67	1.36	6.3	6.3	25	1.5	4.5	0	8.45~70.8
i	150	0.67	1.36	6.3	6.3	25	1.5	2	0	0~37.9

* The viscosity of oil phase was too high to be dispersed.

** Dispersion coagulated

Table 4-2 The effect of curing time on Tg of epoxy particles

Curing Time (hr)	**Tg(°C)**
4.5	61.06
2	47.05

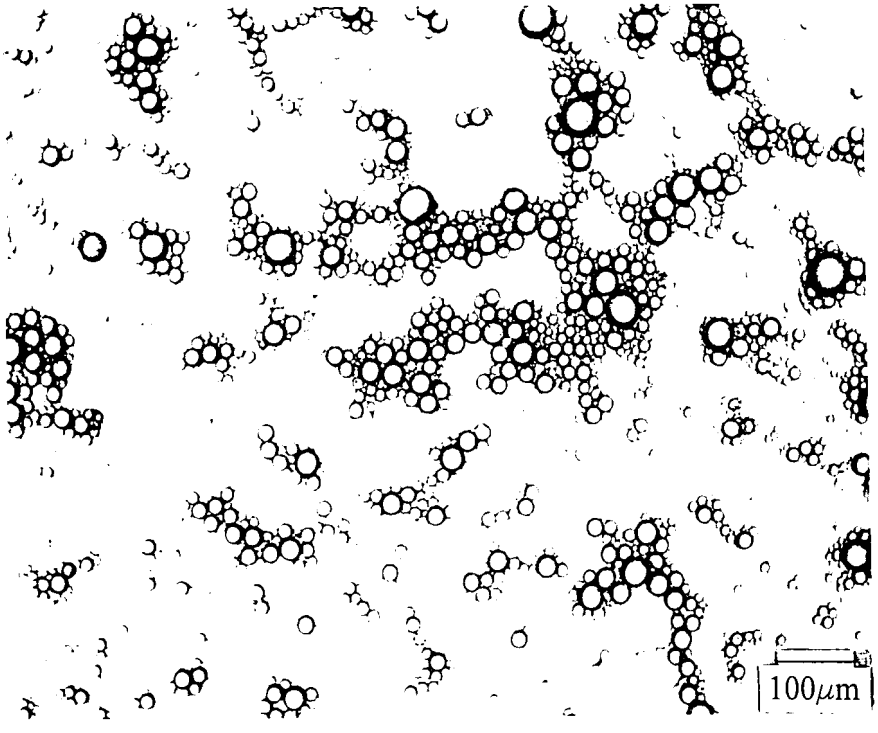

Fig. 4-2 TOM photograph of the epoxy particles generated in batch **h**

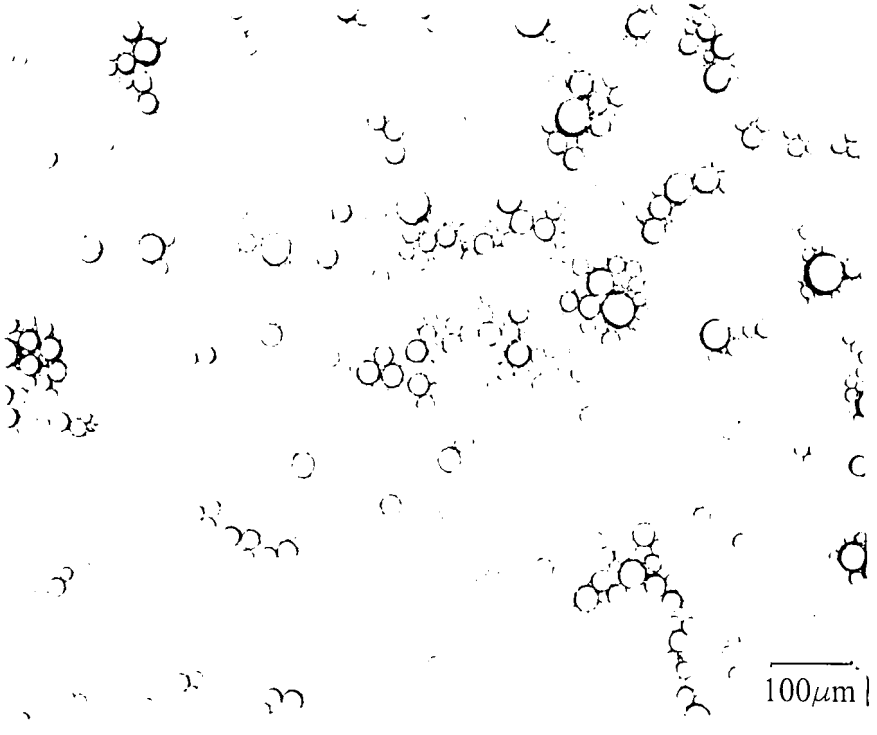

Fig. 4-2 TOM photograph of the epoxy particles generated in batch **h**

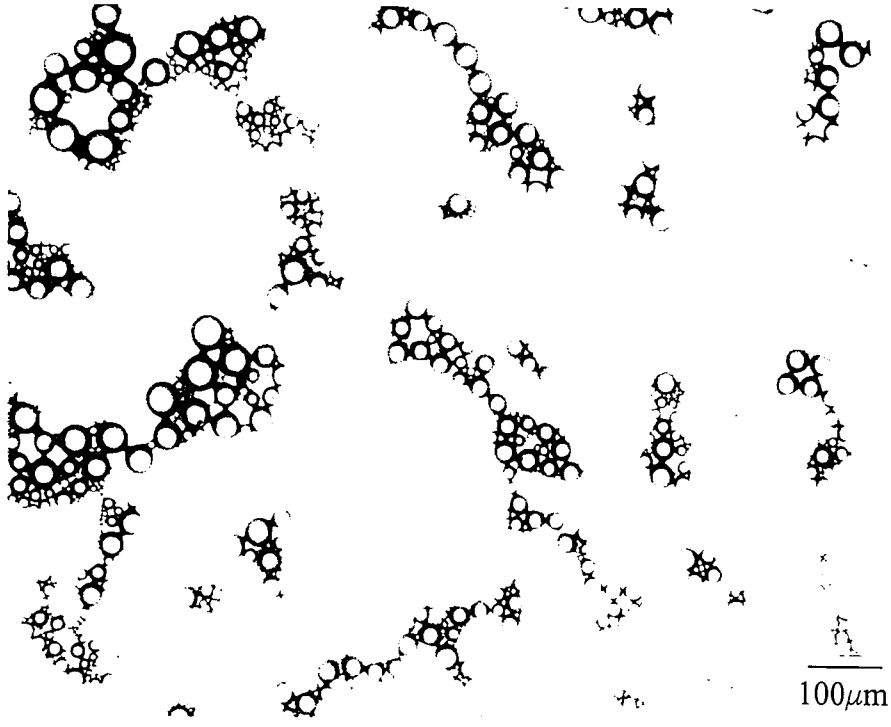

Fig. 4-3 TOM photograph of the epoxy particles generated in batch **i**

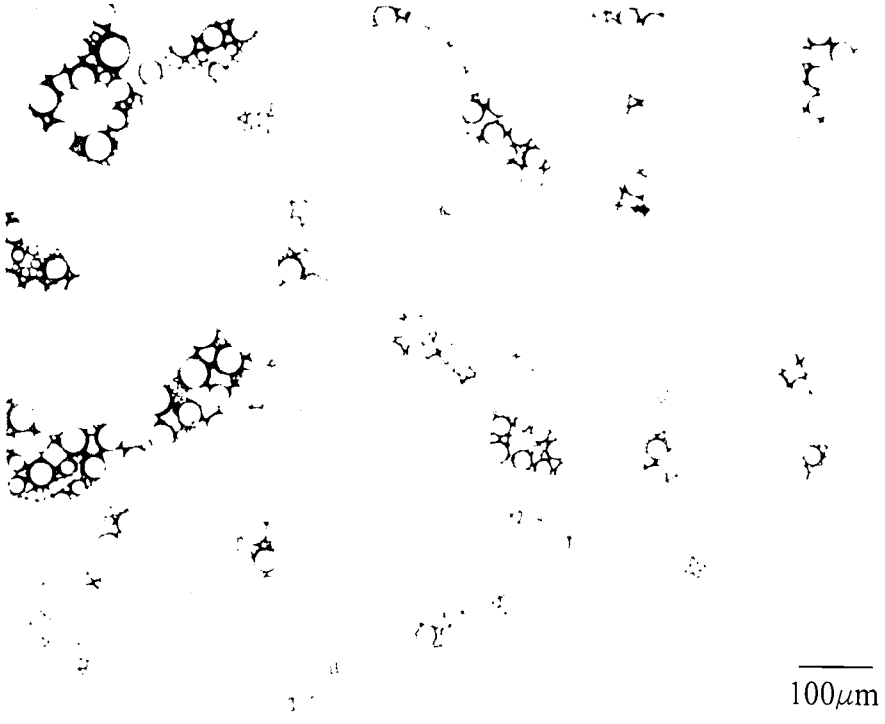

Fig. 4-3 TOM photograph of the epoxy particles generated in batch **i**

4.2 THE EFFECT OF CURING SCHEDULE

The fracture toughness of rubber-modified polymers depends on the properties of the dispersed rubber phase. However, the properties of the rigid matrix are even more important, since the plastic processes responsible for toughening take place in within the matrix. The influence of matrix ductility on fracture toughness has been reported by many investigators[7,16,35-40].

Wu[16] claimed that at the same amount of rubber, the extent to which a matrix can be rubber toughened depends on the intrinsic brittleness/ductility of the matrix polymer. Pearson and Yee[39] varied the matrix ductility by using epoxide resins of varying epoxide monomer molecular weights. These researchers found that the fracture toughness values for the neat epoxies are almost independent of the monomer molecular weight of the epoxide resin used. However, the fracture toughness values of the elastomer-modified epoxies are very dependent on the epoxide monomer molecular weight[39](Fig. 4-4). The toughenability of a DGEBA epoxy by elastomeric addition depends upon the crosslink density of the epoxy matrix. The lower the crosslink density (the higher the monomer molecular weight), the greater the toughenability[39]. These researchers also concluded that simply adding a soft elastomeric phase does not guarantee enhanced toughness. However, the addition of a soft elastomeric phase to a ductile matrix results in the desired toughness enhancement[39].

Some investigators used the changing of curing schedule to vary the crosslink density[36-38,40]. By employing different curing schedules the degree of crosslinking in the matrix phase can be changed, but without altering the microstructure of the dispersed rubbery phase. Levita[40] showed that the fracture toughness of Epon828-piperidine increases on increasing curing temperature(Fig. 4-5). It shows that the networks obtained at high temperature are looser and more flexible, as suggested by the progressive reduction of the glass transition temperature(Fig.4-6).

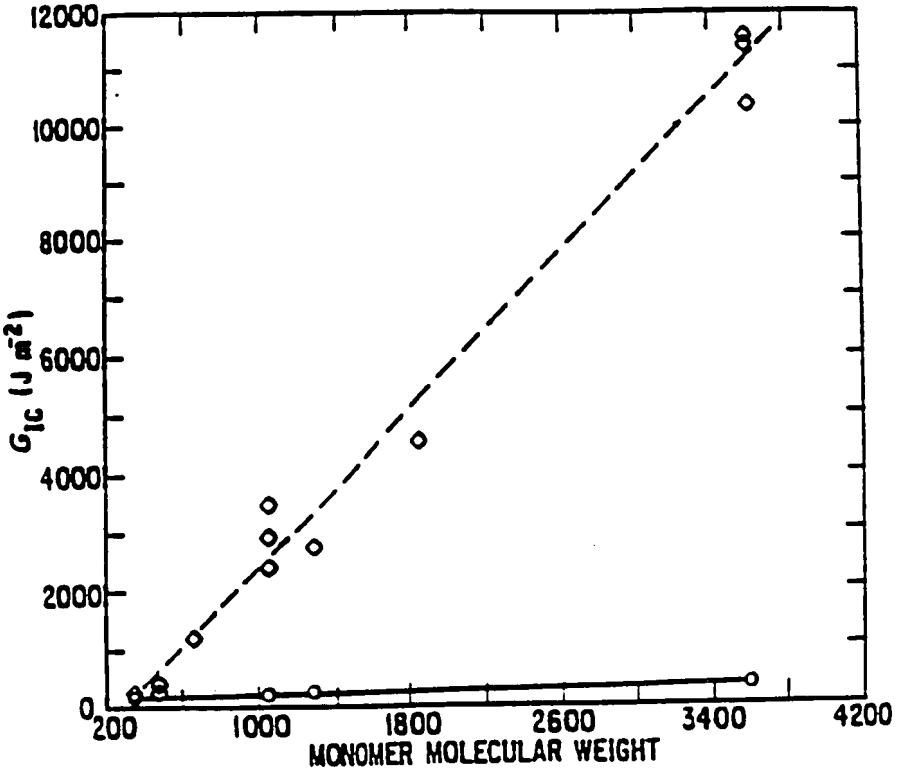

Fig. 4-4 Fracture toughness increases modestly with increasing monomer molecular weight for neat epoxies. However, the fracture toughness of the rubber-modified epoxies increases dramatically with increasing epoxide monomer molecular weight. (◊) Elastomer-modified resins ; (○) neat resins[39]

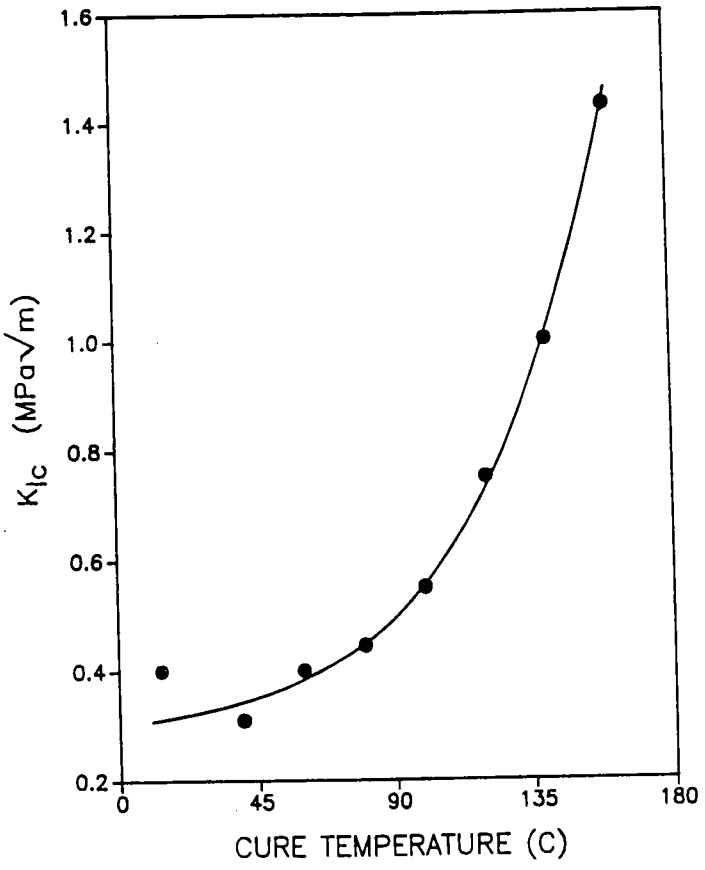

Fig. 4-5 Fracture toughness, K_{IC}, of the Epon 828-piperidine resin as a function of cure temperature. The fracture toughness increases on increasing curing temperature. It shows that the networks obtained at high temperatures are looser and more flexible.[40]

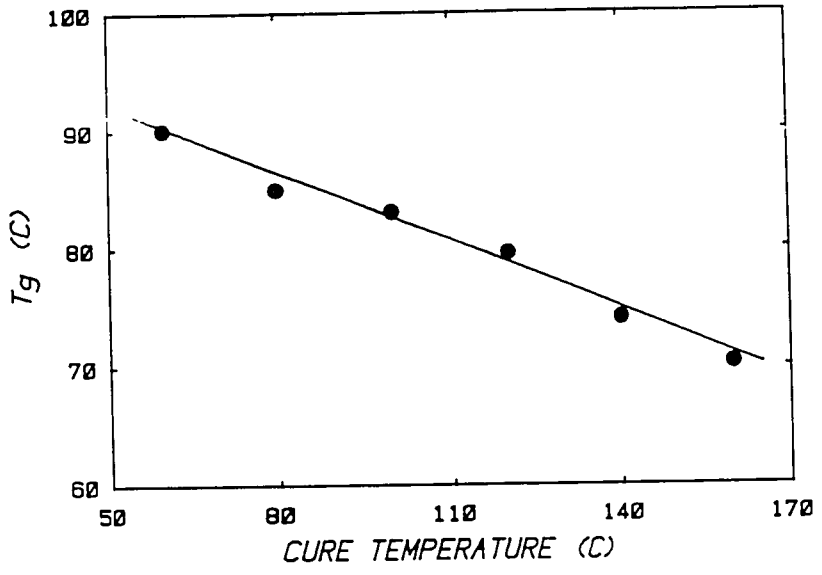

Fig. 4-6 Glass-transition temperature of the Epon 828-piperidine resin as a function of cure temperature. The Tg decreases as the cure temperature increases. It shows that high cure temperatures result in lower cross-link densities.[40]

According to the information above we can know that the fracture toughness of rubber-modified epoxies depends on the ductility of the matrix and the toughenability increases as the ductility of the matrix increases. This is very important to the development of the curing schedule in our research.

Table 4-3 lists the K_{IC} and Tg of neat and rubber-modified epoxies cured by different curing schedule. The original curing schedule for neat and rubber-modified epoxies is 120° C 16 hours. However, since we cure the epoxy particles at 80° C, we have to use two step curing schedule. The curing schedule **b** is 80° C 4.5 hours and 120° C 16 hours since we first successfully generate epoxy particles by cured the oil phase at 80° C for 4.5 hours. However, the result of curing schedule **b** shows that the ductility of the matrix is too low (high Tg) and the fracture toughness difference between inter-connected and uniformly dispersed structures is only 0.17. We have to find a suitable curing schedule to get a ductile matrix to increase the difference of fracture toughness so that we can study the influence of the dispersion of rubbery phase. According to Levita[40], the ductility of the matrix increases as the curing temperature increases. So, in curing schedule **c** we use 80° C 4.5 hours and 160° C 6 hours. The results show that the matrix is more ductile and more toughenable than that for curing schedule **b**. Curing schedule **d** is 80° C 2 hours and 120° C 16 hours. The results show that the matrix is not ductile enough again. Curing schedule **e** is 80° C 2 hours and 160° C 6 hours. The results show that the matrix is sufficiently ductile and the difference of the fracture toughness of inter-connected and uniformly dispersed structures increased to 0.47.

The 80° C 2 hours and 160° C 6 hours curing schedule was used for the curing of the models and original systems in Section 4.3.

Table 4-3 The effect of curing schedule on K_{IC} and Tg of neat and rubber-modified epoxies

Sample ID	Curing Schedule (hr)	Neat Epoxy		MBS*/Epoxy		MBS-COOH/Epoxy	
		K_{IC}**	Tg	K_{IC}	Tg	K_{IC}	Tg
a	120 (16)	0.67	89.9	2.58	90.0	2.15	90.6
b	80 (4.5), 120 (16)	0.78	100.4	1.89	94.3	1.72	92.3
c	80 (4.5), 160(6)	0.55	87.4	2.45	87.3	2.08	89.4
d	80 (2), 120(16)	0.69	89.8	2.23	90.7	1.94	92.0
e	80 (2), 160(6)	0.65	85.1	3.00	83.9	2.53	83.0

* EXL-2691 from Rohm & Haas

** $Mpa.m^{1/2}$, Fracture toughness results were get from SEN-3PB fracture toughness tests.

4.3 THE EFFECT OF BLEND MORPHOLOGY

4.3.1 Rubber/Epoxy particles/Epoxy System(model I)

25wt% epoxy particles of the total epoxy was used to generate this system. Higher wt% of epoxy particles was tried, but the viscosity of the system was too high for mechanical stirring. MBS(RJC-2680) rubber was used since the dispersion of them in the epoxy matrix is better than that of the MBS-COOH(EXL-2611). Fig. 4-7 and Fig. 4-8 are the SEM micrographs taken from the stress-whitened zone of epoxies modified by EXL-2611 and RJC-2680, respectively. The dispersion of the RJC-2680 modified epoxy is much more uniformly than that of EXL-2611 modified epoxy. 10wt% rubber particles of the total epoxy(epoxy particles + liquid epoxy) was used. For comparison, a batch without epoxy particles was made.

Fig. 4-9 and Fig. 4-10 are the SEM micrographs taken from the stress-whitened zone of the model system. We can see that the epoxy particles still retain their shapes and more importantly, the interfaces between the epoxy particles and the matrix epoxy do not interference with the crack propagation. Table 4-4 lists the results of the SEN-3PB fracture toughness tests and the yield stress results from the compression tests of the model system and the original system.

Table 4-4 Mechanical properties of the original system and the model(model I) system

	K_{1C} ($MPa.m^{1/2}$)	σ_y (MPa)
Original System*	1.98	87.97
Model System**	2.09	81.92

* The rubber content is 10 wt% of the epoxy.

** The rubber content is 10 wt% of the total epoxy. 25 wt% of the total epoxy is epoxy particles.

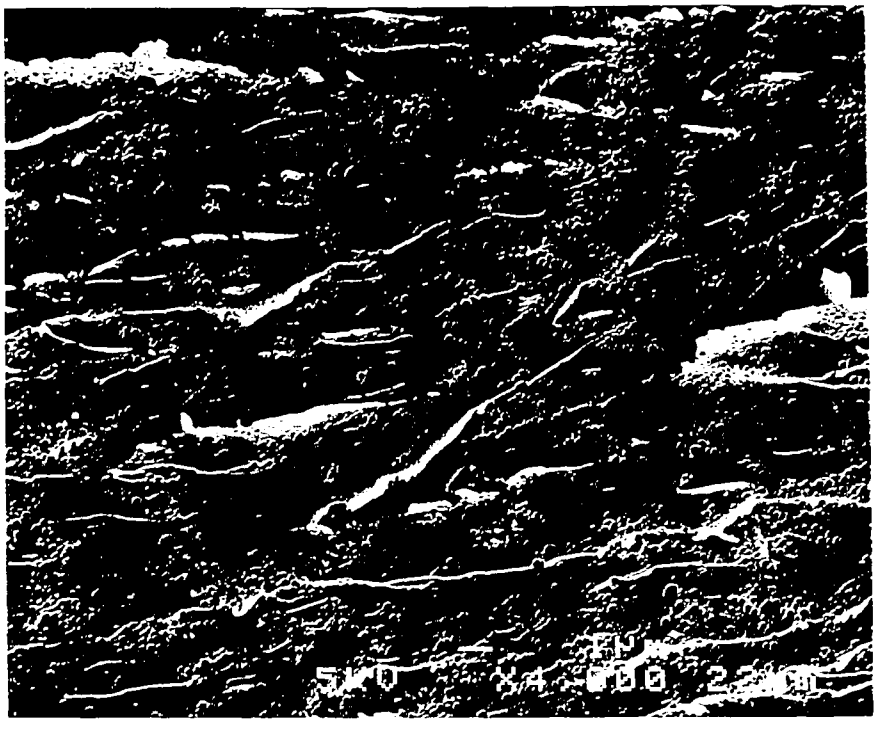

Fig. 4-7 SEM micrograph taken from the stress-whitened zone of epoxy modified by EXL-2611. The rubber particles do not disperse uniformly.

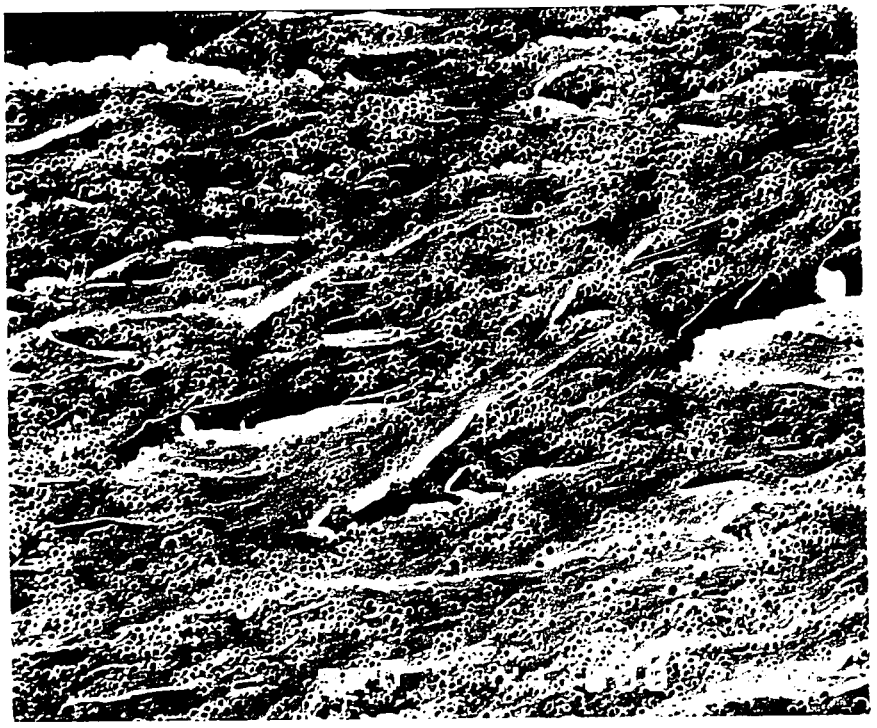

Fig. 4-7 SEM micrograph taken from the stress-whitened zone of epoxy modified by EXL-2611. The rubber particles do not disperse uniformly.

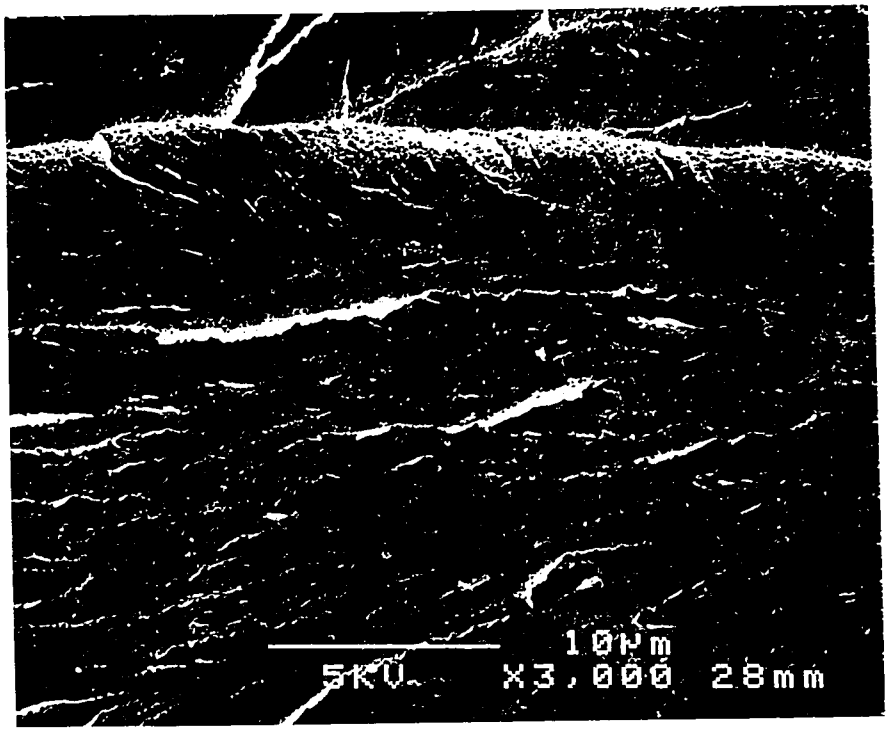

Fig. 4-8 SEM micrograph taken from the stress-whitened zone of epoxy modified by RJC-2680. The rubber particles disperse very uniformly.

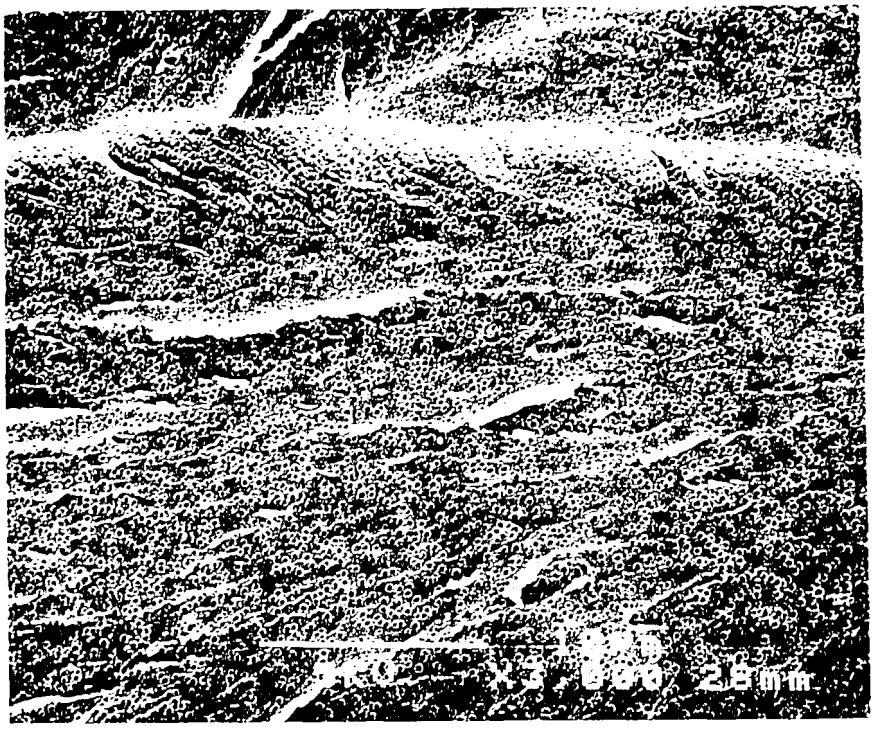

Fig. 4-8 SEM micrograph taken from the stress-whitened zone of epoxy modified by RJC-2680. The rubber particles disperse very uniformly.

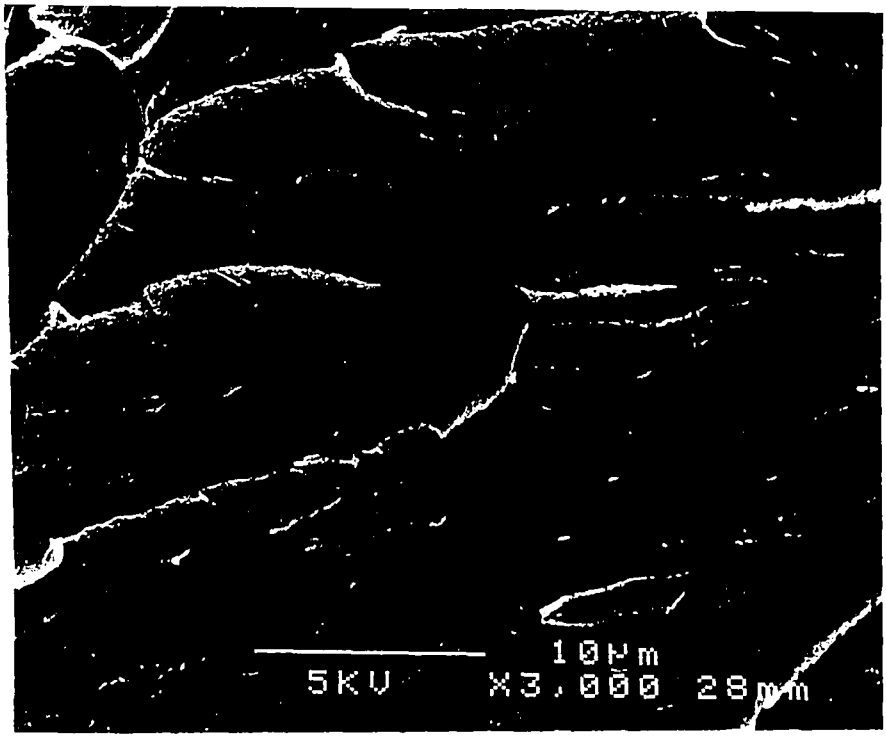

Fig. 4-9 SEM micrograph taken from the stress-whitened zone of the model system(model I). As seen in this figure, the interfaces between epoxy particles and epoxy matrix do not interference with the crack propogation.

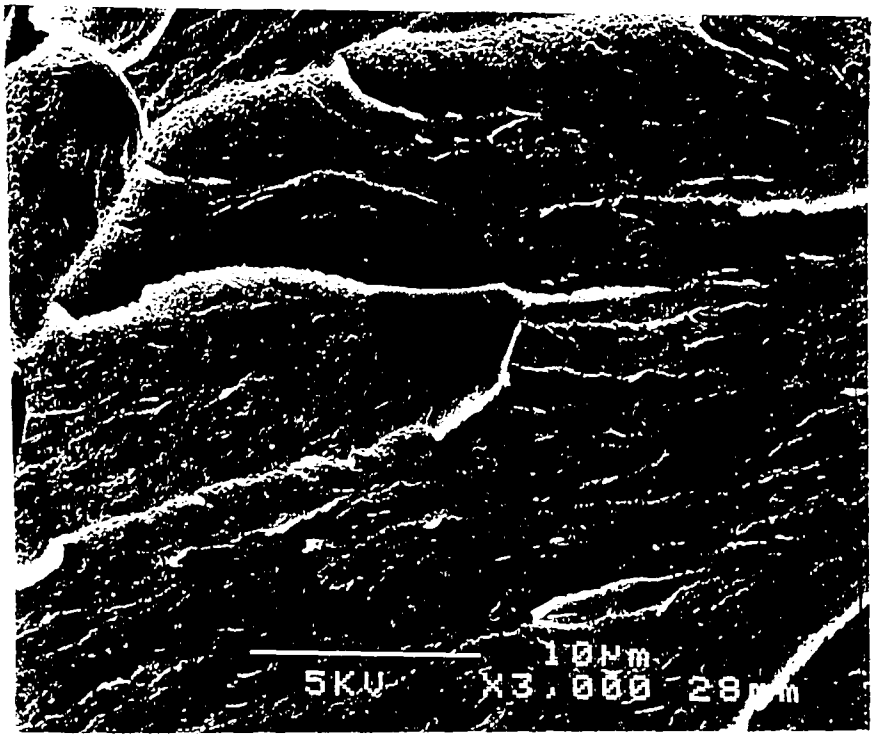

Fig. 4-9 SEM micrograph taken from the stress-whitened zone of the model system(model I). As seen in this figure, the interfaces between epoxy particles and epoxy matrix do not interference with the crack propogation.

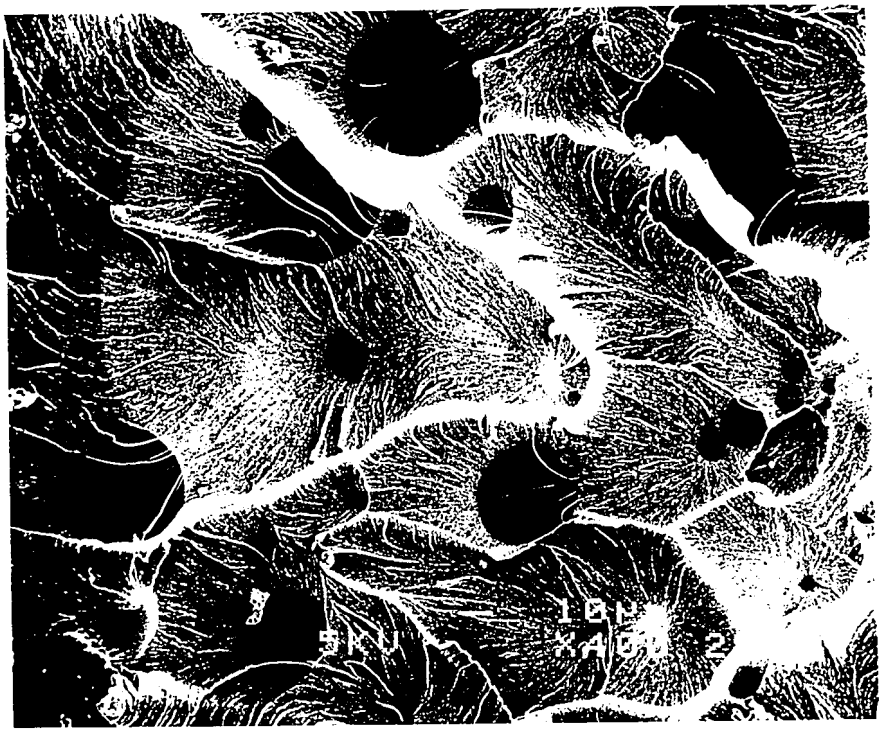

Fig. 4-10 SEM micrograph taken from the stress-whitened zone of the model sysytem(model I). The epoxy particles still retain their shapes and the interfaces between epoxy particles and epoxy matrix do not interference with the crack propogation.

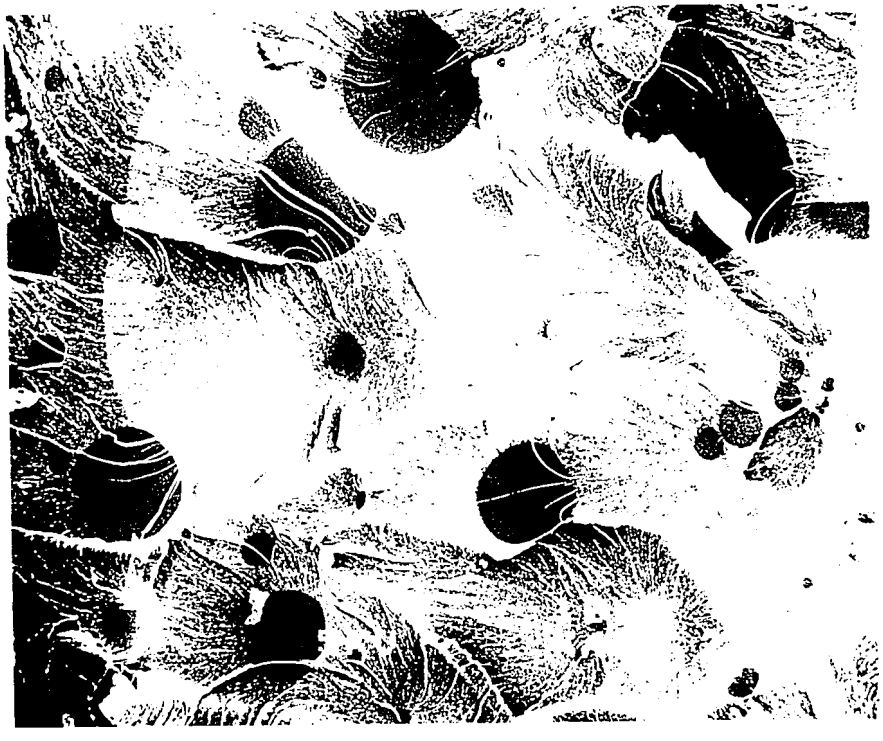

Fig. 4-10 SEM micrograph taken from the stress-whitened zone of the model sysytem(model I). The epoxy particles still retain their shapes and the interfaces between epoxy particles and epoxy matrix do not interference with the crack propogation.

The results show that for the model system, the fracture toughness is somewhat higher and the yield stress is lower. Therefore the toughness of the original system can indeed be improved if we add some pre-gelled epoxy particles into the system. Moreover the toughness of the system can be improved only if we increase the connectivity of the rubber particles.

Fig. 4-11shows the fracture surfaces of the model system(left) and the original system(right). We can see that the deformation zone(stress-whitened zone) of the model system is larger than that of the original system. It also means that the increase of the connectivity of the rubber particles can improve the toughness of the blend.

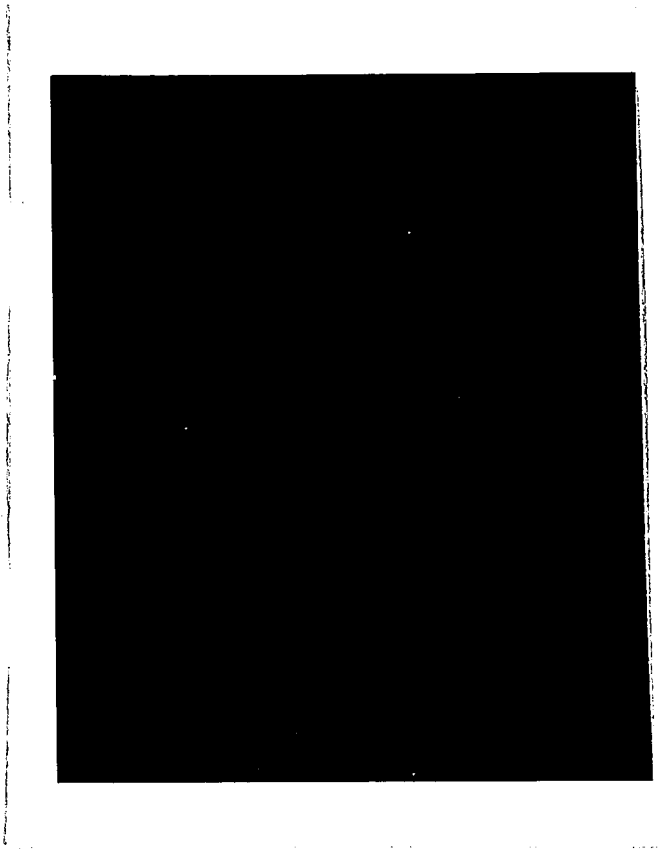

Fig. 4-11 The fracture surfaces of the model system(left) and the original system(right).The stress-whitened zone of the model system is larger than that of the original system.

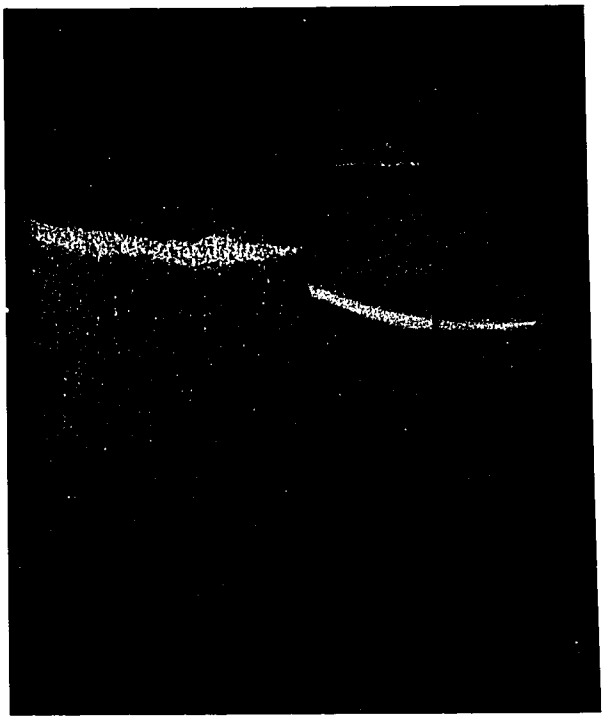

Fig. 4-11 The fracture surfaces of the model system(left) and the original system(right).The stress-whitened zone of the model system is larger than that of the original system.

4.3.2 Epoxy Particles(with rubber particles in them)/Epoxy System(model II)

10 wt% rubber particles was used for the fabrication of the epoxy particles. Higher wt% of rubber particles has been tried, but the viscosity of the system was too high for mechanical stirring. The weight of the pre-gelled epoxy(weight of epoxy particles - weight of rubber particles) is 25 wt% of the total epoxy. RJC-2680 rubber was also used in this research. For comparison, a batch without epoxy particles was made.

Fig. 4-12 and Fig.4-13 are SEM micrographs taken from the fracture surface of the model system. We can see that the epoxy particles still retain their shapes and rubber particles can be embedded into the epoxy particles to control the clustering of rubber particles in the epoxy matrix.

Table 4-5 lists the results of the SEN-3PB fracture toughness tests and the yield stress results from the compression tests of the model system and the original system.

Table 4-5 Mechanical properties of the original system and the model(model II) system

	K_{1C} ($MPa.m^{1/2}$)	σ_y (MPa)
Original System*	1.07	99.0
Model System**	0.89	99.1

* The rubber content is 2.5 wt% of the epoxy.

** The rubber content is 10 wt% of the epoxy particles. 25 wt% of the total epoxy is epoxy particles.

From the results above we can see that for the model system, the fracture toughness is somewhat lower and the yield stress is similar to that of the original system. These results suggest that clustering may be a necessary but not a sufficient requirement to increase the fracture toughness of the rubber-modified epoxies. Clearly, there is support for the

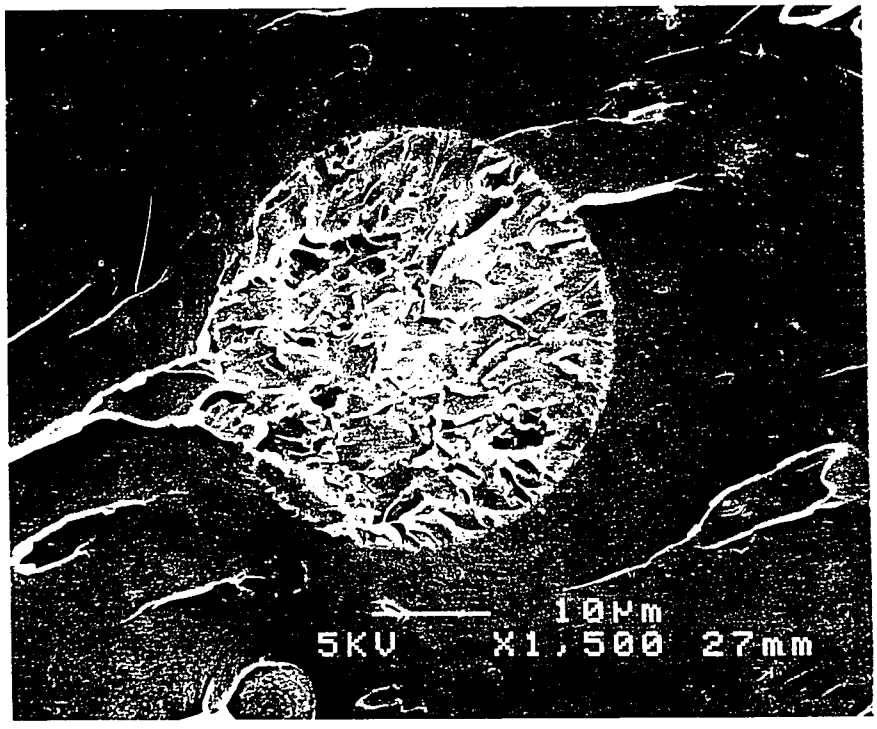

Fig. 4-12 SEM micrograph taken from the fracture surface of the model system(model II). It shows that the rubber particles can be embedded into the epoxy particles to control the clustering of the rubber particles in the epoxy matrix.

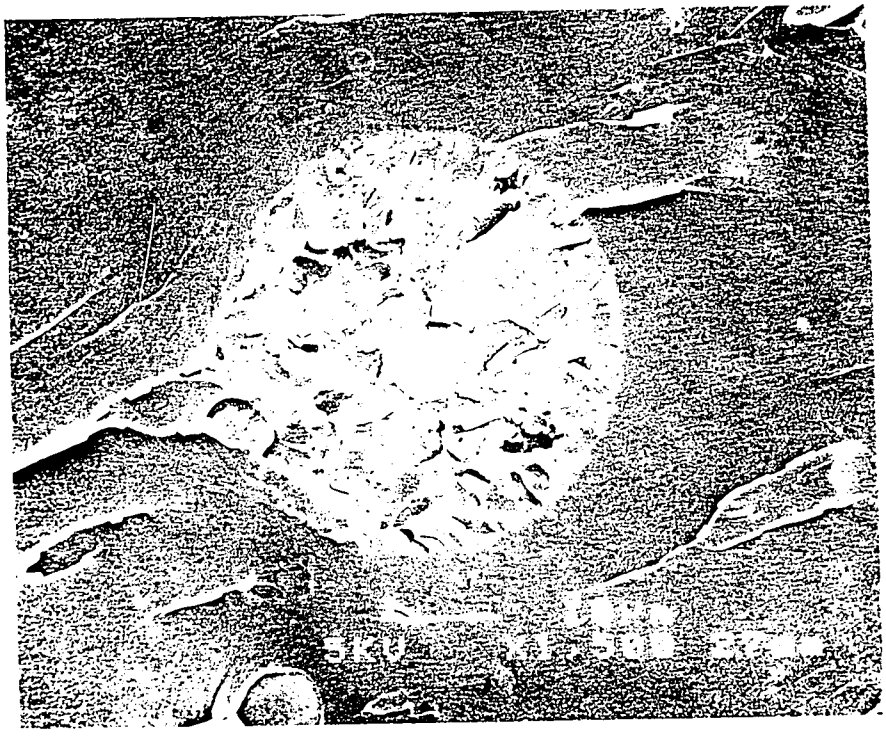

Fig. 4-12 SEM micrograph taken from the fracture surface of the model system(model II). It shows that the rubber particles can be embedded into the epoxy particles to control the clustering of the rubber particles in the epoxy matrix.

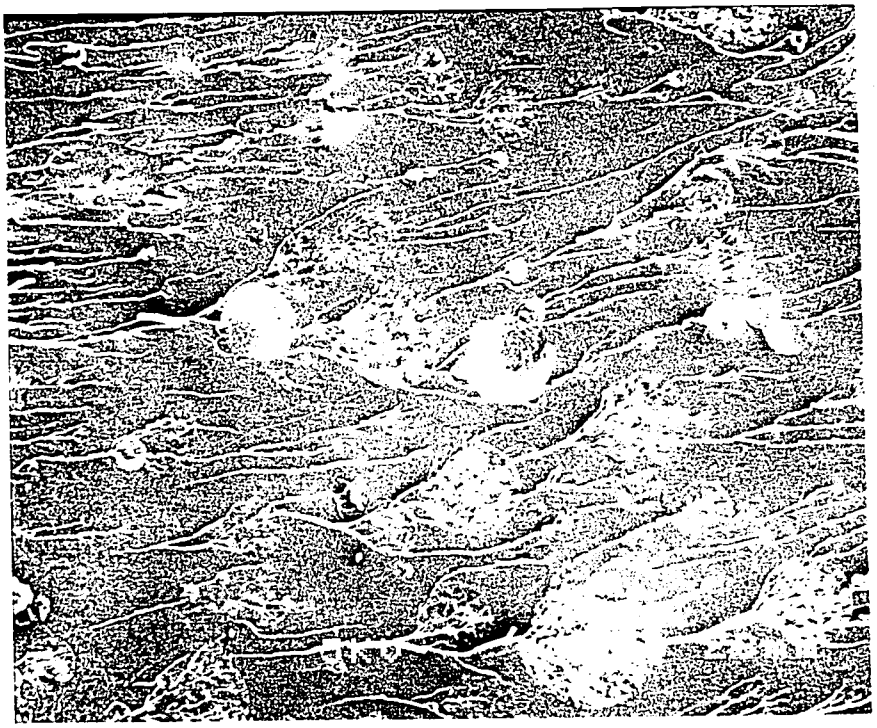

Fig. 4-13 SEM micrograph taken from the fracture surface of the model system(model II). As seen in this figure, the epoxy particles still retain their shapes. It also shows that the rubber particles can be embedded into the epoxy particles to control the clustering of the rubber particles in the epoxy matrix.

Fig. 4-13 SEM micrograph taken from the fracture surface of the model system(model II). As seen in this figure, the epoxy particles still retain their shapes. It also shows that the rubber particles can be embedded into the epoxy particles to control the clustering of the rubber particles in the epoxy matrix.

conclusion that a co-continuous morphology is also required.

One important point of this research is that the epoxy particles is only 25 wt% of the total epoxy. Obviously, in order to effectively correlate the connectivity and clustering of the rubber particles to the fracture toughness performance, higher amount of the epoxy particles is needed. So that the rubber particles are forced to segregate or cluster without significantly reducing the connectivity.

5. CONCLUSIONS AND RECOMMENDATIONS

In this research, we have proposed two models to control the blend morphology of the rubber-toughened epoxies, one is rubber/epoxy particles/epoxy system(model I) which addresses the connectivity issue, the other one is epoxy particles(with rubber particles in them)/epoxy system(model II) which addresses the clustering issue. The results showed that pre-gelled epoxy particles can be added to force the rubber particles to segregate and rubber particles can be embedded into the epoxy particles to control the size of the micro-clusters of the rubber particles.

These results also show that the connectivity of the rubber particles in the epoxy matrix might be very important to the fracture toughness performance of the rubber-modified epoxies, but further research is needed.

In this research, the amount of the epoxy particles added were only 25wt% since the viscosity limit for the mechanical stirring. In order to further understand the effect of the blend morphology to the toughening performance, higher amount of the epoxy particles is desirable. One can use some solvent to overcome the viscosity problem of the processing to increase the amount of epoxy particles.

More control to the epoxy particle size is suggested. One can use screen meshes to control the size of the epoxy particles.

One might be get more insight of the effect of the blend morphology to the fracture toughness performance of rubber-toughened epoxies by using more and size controlled epoxy particles.

6. REFERENCES

1. R. Bagheri, *Ph.D. Dissertation*, Lehigh University (1995).

2. J. Y. Qian, *Ph.D. Dissertation*, Lehigh University (1994).

3. I. C. Huang, *Ph.D. Dissertation*, University of Michigan (1994).

4. A. F. Yee and R. A. Pearson, *J. of Materials Science*, **21**, 2462 (1986).

5. S. Y. Hobbs, M. E. J. Dekkers, and V. H. Watkins, *ibid*, 2025 (1988).

6. R. J. M. Borggreve, R. J. Gaymans, J. Schuijer and J. F. Ingen Housz, *Polymer*, **28**, 1489 (1987).

7. A. J. Kinloch, and D. L. Hunston, *J. of Materials Science Letters*, **5**, 909 (1986).

8. B. Bagheri, P. C. Hung, R. A. Pearson, and A. Voloshin, *Polymer Interfaces Center Research Progress Report,* **No. 6**, 118 (1994).

9. I. Vallo, L. Hu, P. M. Frontini, and R. J. J. Williams, *ibid*, 2481 (1993).

10. A. C. Grillet, J. Galy, and J. P. Pascault, *Polymer*, **33**, 34 (1992).

11. D. Verchere, H. Sautereau, J. P. Pascault, S. M. Moschiar, C. C. Riccardi, and R. J. J. Williams, *Advances in Chemistry Series*, **233**, 335 (1993).

12. A. J. Kinloch, *Advances in Chemistry Series*, **222**, 67 (1987).

13. W. D. Bascom, and D. L. Hunston, *Advances in Chemistry Series*, **222**, 135 (1987).

14. S. Wu, *Polymer*, **26**, 1855 (1985).

15. J. N. Sultan and F. J. McGarry, *Polymer Engineering and Science*, **13**, 29 (1973).

16. S. Wu, *Polymer Engineering and Science*, **30**, 753 (1990).

17. R. A. Pearson and A. F. Yee, *J. of Materials Science,* **26**, 3828 (1991).

18. S. Kunz-Douglass, P. W. R. Beaumont and M. F. Ashby, *ibid*, **15**, 1109 (1980).

19. W. D. Bascom, R. Y. Ting, R. J. Moulton, C. K. Riew, and A. R. Siebert, *J. of Materials Science*, **16**, 2657 (1981).

20. T. K. Chen and Y. H. Jan, *J. of Materials Science*, **27**, 111 (1992).

21. A. Margolina, and S. Wu, *Polymer*, **29**, 2170 (1988).

22. G. Cigna, P. Lomellini, and M. Merlotti, *J. of Applied Polymer Science*, **37**, 1527 (1989).

23. K. Yamanaka and T. Inoue, *Polymer*, **30**, 662 (1989).

24. K. Yamanaka, Y. Takagi, and T. Inoue, *Polymer*, **60**, 1839 (1989).

25. H. Tanaka, T. Hayashi, and T. Nishi, *J. of Applied Physics*, **65**, 4480 (1989).

26. A. H. Thiessen, J. C. Alter, *Monthly Weather Review*, **39**, 1082 (1911).

27. R. E. Horton, *Engineering News-Record*, 221 (1917).

28. Y. C. Huang and R. A. Pearson, *Polymer Interfaces Center Research Progress Report,* **No. 9**, 123 (1996).

29. *Water-Base Coatings*, Technical Report AFML-TR-74-208, Part I (1974).

30. M. Sambasivem, *Ph.D. Dissertation*, Lehigh University (1995).

31. ASTM D5045, *Standard Test Method for Plane Strain Fracture Toughness and Strain Engery Release Rate of Plastic Materials*, Annual Book of ASTM Standards, ASTM, Philadelphia, PA (1991).

32. ASTM D695, *Standard Test Method for Compressive Properties of Rigid Plastics*, Annual Book of ASTM Standards, ASTM, Philadelphia, PA (1991).

33. M. S. El-Aasser, *26th Annual Short Course of Emulsion Polymers Institute*, **3** (1995).

34. E. G. Bozzi and C. Y. Zendig, *American Chemical Society*, **114**, 71 (1978).

35. W. L. Bradley, W. Schultz, C. Corleto, and S. Komatsu, *Advances in Chemistry Series*, **233**, 317 (1993).

36. S. J. Shaw, and D. A. Tod, *J. of Adhesion*, **28**, 231 (1989).

37. G. Levita, S. D. Petris, A. Marchetti and A. Lazzeri, *J. of Materials Science*, **26**, 2348 (1991).

38. A. J. Kinloch, C. A. Finch, and S. Hashemi, *Polymer Communications*, **28**, 322 (1987).

39. R. A. Pearson and A. F. Yee, *J. of Materials Science*, **24**, 2571 (1989).

40. G. Levita, *Advances in Chemistry Series*, **222**, 93 (1987).

VITA

Ying-Chieh Huang was born to Cheng-Tzer Huang and Mei-Fen Shieh on September 5, 1971 in Pingtung, Taiwan, R.O.C.

He received his B.E. in Materials Science from Feng Chia University(Taichung, Taiwan, R.O.C.) in June 1993.

He received the Indicated Subject Scholarship for the course "Introduction to Materials Science" in 1990 and received some scholarships for his excellent performance in academic during 1990~1993.

He worked for Delta FRP Mfg. Inc., (FRP : Fiber Reinforced Plastics) from 07/91 to 08/91 and worked for Carbon Fiber Laboratory in Feng Chia University from 02/92 to 01/93.

He joined the Materials Science and Engineering department of Lehigh University in 08/94 and joined Polymer Interfaces Center in 05/95 under the direction of Dr. R. A. Pearson.

END OF TITLE